NASA/TP—2009–216061

Sunspot Activity Near Cycle Minimum and What It Might Suggest for Cycle 24, the Next Sunspot Cycle

Robert M. Wilson and David H. Hathaway
Marshall Space Flight Center, Marshall Space Flight Center, Alabama

September 2009

The NASA STI Program…in Profile

Since its founding, NASA has been dedicated to the advancement of aeronautics and space science. The NASA Scientific and Technical Information (STI) Program Office plays a key part in helping NASA maintain this important role.

The NASA STI Program Office is operated by Langley Research Center, the lead center for NASA's scientific and technical information. The NASA STI Program Office provides access to the NASA STI Database, the largest collection of aeronautical and space science STI in the world. The Program Office is also NASA's institutional mechanism for disseminating the results of its research and development activities. These results are published by NASA in the NASA STI Report Series, which includes the following report types:

- TECHNICAL PUBLICATION. Reports of completed research or a major significant phase of research that present the results of NASA programs and include extensive data or theoretical analysis. Includes compilations of significant scientific and technical data and information deemed to be of continuing reference value. NASA's counterpart of peer-reviewed formal professional papers but has less stringent limitations on manuscript length and extent of graphic presentations.

- TECHNICAL MEMORANDUM. Scientific and technical findings that are preliminary or of specialized interest, e.g., quick release reports, working papers, and bibliographies that contain minimal annotation. Does not contain extensive analysis.

- CONTRACTOR REPORT. Scientific and technical findings by NASA-sponsored contractors and grantees.

- CONFERENCE PUBLICATION. Collected papers from scientific and technical conferences, symposia, seminars, or other meetings sponsored or cosponsored by NASA.

- SPECIAL PUBLICATION. Scientific, technical, or historical information from NASA programs, projects, and mission, often concerned with subjects having substantial public interest.

- TECHNICAL TRANSLATION. English-language translations of foreign scientific and technical material pertinent to NASA's mission.

Specialized services that complement the STI Program Office's diverse offerings include creating custom thesauri, building customized databases, organizing and publishing research results…even providing videos.

For more information about the NASA STI Program Office, see the following:

- Access the NASA STI program home page at <http://www.sti.nasa.gov>

- E-mail your question via the Internet to <help@sti.nasa.gov>

- Fax your question to the NASA STI Help Desk at 443–757–5803

- Phone the NASA STI Help Desk at 443–757–5802

- Write to:
  NASA STI Help Desk
  NASA Center for AeroSpace Information
  7115 Standard Drive
  Hanover, MD 21076–1320

NASA/TP—2009–216061

Sunspot Activity Near Cycle Minimum and What It Might Suggest for Cycle 24, the Next Sunspot Cycle

Robert M. Wilson and David H. Hathaway
Marshall Space Flight Center, Marshall Space Flight Center, Alabama

National Aeronautics and
Space Administration

Marshall Space Flight Center • MSFC, Alabama 35812

September 2009

Available from:

NASA Center for AeroSpace Information
7115 Standard Drive
Hanover, MD 21076–1320
443–757–5802

This report is also available in electronic form at
<https://www2.sti.nasa.gov>

TABLE OF CONTENTS

LIST OF FIGURES

LIST OF FIGURES (Continued)

LIST OF TABLES

LIST OF ACRONYMS

12-mma	12-month moving average
ASC	ascent duration in months, equal to t(Rm–RM)
MSFC	Marshall Space Flight Center
N	North latitude
NASA	National Aeronautics and Space Administration
NOAA	National Oceanic and Atmospheric Administration
RGO	Royal Greenwich Observatory
S	South latitude
SOON	Solar Optical Observing Network
USAF	United States Air Force

NOMENCLATURE

A	12-mma of monthly mean sunspot area
$(A/G)m$	minimum value of the 12-mma of A/G
$(A/G)M$	maximum value of the 12-mma of A/G
Am	minimum value of the 12-mma of A
AM	maximum value of the 12-mma of A
cl	confidence level
$E((A/G)m)$	epoch of occurrence of $(A/G)m$
$E((A/G)M)$	epoch of occurrence of $(A/G)M$
$E(Am)$	epoch of occurrence of Am
$E(AM)$	epoch of occurrence of AM
$E(FHLS)$	epoch of occurrence of $FHLS$
$E(Gm)$	epoch of occurrence of Gm
$E(GM)$	epoch of occurrence of GM
$E(Hm)$	epoch of occurrence of Hm
$E(HM)$	epoch of occurrence of HM
$E(Lm)$	epoch of occurrence of Lm
$E(LM)$	epoch of occurrence of LM
$E(Rm)$	epoch of occurrence of Rm
$E(RM)$	epoch of occurrence of RM
$E(SM)$	epoch of occurrence of SM

NOMENCLATURE (Continued)

f	number of individual sunspots
FHLS	month of first high-latitude spot occurrence
FSD	month of first spotless day occurrence
g	number of groups
G	12-mma of monthly mean number of groups
g(*h*)/*g*	ratio of monthly mean number of high-latitude groups to monthly mean number of groups
Gm	minimum value of the 12-mma of *G*
GM	maximum value of the 12-mma of *G*
H	12-mma of highest latitude spot
Hm	minimum value of the 12-mma of *H*
HM	maximum value of the 12-mma of *H*
k	correction factor
L	12-mma of weighted mean latitude of sunspots
LLLS	month of last low-latitude spot occurrence
Lm	minimum value of the 12-mma of *L*
LM	maximum value of the 12-mma of *L*
LSD	month of last spotless day occurrence
n	sunspot cycle number
P	probability
P(0.5–0.5)	period in months between occurrences of *g*(*h*)/*g* >0.5 of successive cycles
P(*Am*–*Am*)	period in months between *Am* occurrences of successive cycles

NOMENCLATURE (Continued)

P(*AM*–*AM*)	period in months between *AM* occurrences of successive cycles
P(*FSD*–*FSD*)	period in months between *FSD* occurrences of successive cycles
P(*Gm*–*Gm*)	period in months between *Gm* occurrences of successive cycles
P(*GM*–*GM*)	period in months between *GM* occurrences of successive cycles
P(*Hm*–*Hm*)	period in months between *Hm* occurrences of successive cycles
P(*HM*–*HM*)	period in months between *HM* occurrences of successive cycles
P(*Lm*–*Lm*)	period in months between *Lm* occurrences of successive cycles
P(*LM*–*LM*)	period in months between *LM* occurrences of successive cycles
P(*LSD*–*LSD*)	period in months between LSD occurrences of successive cycles
P(*Rm*–*Rm*)	period in months between *Rm* occurrences of successive cycles
r	coefficient of correlation; relative sunspot number
r^2	coefficient of determination (a measure of the amount of variance explained by the inferred regression)
R	12-mma of monthly mean sunspot number
Rm	minimum value of the 12-mma of R
RM	maximum value of the 12-mma of R
S	12-mma of monthly mean number of spotless days
se	standard error of estimate
sd	standard deviation (also given as σ)
SM	maximum value of the 12-mma of *S*
t(*AM*–*RM*)	elapsed time in months between *AM* and *RM*
t(*FHLS*–*LLLS*)	elapsed time in months between *FHLS* and *LLLS*

NOMENCLATURE (Continued)

t(*FHLS*-*Rm*)	elapsed time in months between *FHLS* and *Rm*
t(*FSD*–*LSD*)	elapsed time in months between *FSD* and *LSD*
t(*FSD*–*Rm*)	elapsed time in months between *FSD* and *Rm*
t(*GM*–*RM*)	elapsed time in months between *GM* and *RM*
t(*Hm*–*Rm*)	elapsed time in months between *Hm* and *Rm*
t(*HM*–*RM*)	elapsed time in months between *HM* and *RM*
t(*Lm*–*Rm*)	elapsed time in months between *Lm* and *Rm*
t(*LM*–*RM*)	elapsed time in months between *LM* and *RM*
t(*Rm*–*HM*)	elapsed time in months between *Rm* and *HM*
t(*Rm*–*LM*)	elapsed time in months between *Rm* and *LM*
t(*Rm*–LSD)	elapsed time in months between *Rm* and LSD
t(*Rm*–*RM*)	elapsed time in months between *Rm* and *RM*
x	independent variable
x^*	modified independent variable
y	dependent variable
y^*	modified dependent variable
σ	standard deviation

TECHNICAL PUBLICATION

SUNSPOT ACTIVITY NEAR CYCLE MINIMUM AND WHAT IT MIGHT SUGGEST FOR CYCLE 24, THE NEXT SUNSPOT CYCLE

1. INTRODUCTION

About 165 yr ago, Samuel Heinrich Schwabe[1] announced that sunspot activity fluctuated with a period of about 10 yr. And so the concept of the sunspot cycle was born. Schwabe determined his finding by counting annually the number of spotless days and the number of 'clusters of spots' (groups) that he observed daily from Dessau, Germany. According to Kiepenheur,[2] Schwabe's result did not receive general attention until several years later when Friedrich Wilhelm Alexander Freiherr von Humboldt mentioned the finding in volume 3 of his 5-volume series *Kosmos*, published between 1845 and 1862 (Humboldt died in 1859). Schwabe, an apothecary by trade, made daily determinations of sunspots for 43 yr, between 1826 and 1868, averaging about 290 observing days per year.[3] Schwabe was awarded the Gold Medal of the Royal Astronomical Society for his achievement in 1857, and in 1868 he was elected a member of the Royal Society.[4,5] He died in 1875 at the age of 85 yr.

Johann Rudolph Wolf, a professional Swiss astronomer, having become aware of Schwabe's discovery, introduced in 1848 his now familiar 'relative sunspot number,' $r=k\ (10g+f)$, where g is the number of sunspot groups, f is the number of individually observed sunspots, and k is a correction factor (originally having a value of 1 as used by Wolf), dependent upon the observer, observing conditions, size of telescope, etc. Wolf also established an international cadre of observers, which continues through today, to monitor the daily changes in r. By piecing together scattered and incomplete older sunspot data, Wolf was able to reconstruct a record of solar activity prior to 1849 (back to 1700 in terms of yearly average estimates, and back to 1610 in terms of estimated epochs of sunspot minimum and maximum), determining the average length of the sunspot cycle to be about 11 yr, rather than 10 yr. The record prior to 1849, however, must be viewed circumspectly, owing to incomplete daily records. [2–8] About 1882, Wolf's successors at Zürich permanently changed the counting method to include the smallest observable spots and weighted spots with penumbrae according to size and umbral structure, employing k=0.60 for the reduction of the new records to the values obtained by Wolf.

In 1874, the Royal Greenwich Observatory (RGO) began routinely (daily) observing the Sun photographically (first introduced by Richard Christopher Carrington), measuring the position of sunspots on the visible solar disk and the sunspot area, both total and umbral areas. (Umbral area refers to the darkest portion of sunspots, whereas total area refers to the overall area of sunspots, including umbral and penumbral areas, as seen in white light.[9]) The RGO, supplemented by observations from Capetown, South Africa, and Kodaikanal, India, continued to record sunspots photographically through 1976, when it concluded its observations. From 1977 onwards, the RGO dataset has been extended using visual observations as reported in the National Oceanic and Atmospheric Administration (NOAA) Space Weather Prediction Center's Preliminary Report and Forecast of Solar Geophysical Data (now called "The Weekly"). The visual observations originate from the United States Air Force (USAF) Solar Optical Observing Network (SOON). The augmented RGO dataset is easily accessible online at the National Aeronautics and Space Administration (NASA) Marshall Space Flight Center (MSFC) solar science website <http://solarscience.msfc.nasa.gov/greenwch.shtml>. Sunspot areas since 1976 have been increased by 40% to compensate for the difference in photographic and visual determinations of sunspot area.[10,11]

Since 1981, the task of computing and maintaining the official record of relative sunspot numbers has been accomplished by the Royal Observatory of Belgium. The record of reliable continuous sunspot observations now spans 160 yr, from January 1849 to the present, although comparison with Douglas V. Hoyt and Kenneth H. Schatten's group sunspot number[12] suggests reliability only since about 1882; i.e., from 1882 the two datasets are virtually identical, but differ, sometimes substantially, prior to 1882. Also, the record of reliable continuous sunspot positions and areas now spans 125 yr, from May 1874 to the present.

The purpose of this NASA Technical Publication (TP) is to examine more closely a number of solar parameters gleaned from the sunspot record, especially how they might relate to cycles 23 and 24, the just ending and beginning sunspot cycles, since some of the parameters are now very near record value, especially as compared to other cycles of the modern era (since about cycle 10).

2. RESULTS AND DISCUSSION

2.1 Parametric Variations Near Cycle Minimum

Figure 1 displays the cyclic variation of the 12-mo moving averages (12-mma; also called the 13-mo running mean or smoothed monthly mean values) of the maximum monthly mean number of spotless days (*SM*, fig. 1(a)), the minimum value of the monthly mean sunspot number (*Rm*, fig. 1(b)), the minimum value of the monthly mean number of sunspot groups (*Gm*, fig. 1(c)), and the minimum value of the monthly mean total sunspot area, corrected for foreshortening and expressed in millionths of the visible solar hemisphere (*Am*, fig. 1(d)). For *SM* and *Rm* the values span cycles 10–24, with tentative values given for cycle 24 (i.e., presuming November 2008 to be the epoch of cycle minimum for cycle 24), while for *Gm* and *Am* the values span cycles 12–24, with tentative values given for cycle 24, as well. Also shown are the medians for each parameter. Hence, for *SM*, *Rm*, *Gm*, and *Am*, respectively, the medians are 19.2, 5.1, 0.56 and 50.9. For *SM*, its tentative value for cycle 24 is now above the median, while for *Rm*, *Gm*, and *Am*, the tentative values for cycle 24 are below their respective medians; i.e., *SM* varies inversely with *Rm*, *Gm*, and *Am*. The purpose of the small arrows for the cycle 24 values is to remind the reader that the values are tentative, presuming cycle 24 minimum in November 2008, and therefore could slightly change as time progresses.

For cycle 24, the tentative value of *SM* (24.2) is the fourth highest, below that of cycles 12 (25.0), 14 (24.3), and 15 (26.2). Similarly, the tentative value of *Rm* (1.8) for cycle 24 is the second smallest, only slightly higher than the value for cycle 15 (1.5); the tentative value of *Gm* (0.20) is tied with cycle 14 as the third smallest, above that of cycles 12 and 15 (both 0.15); and the tentative value of *Am* (7.4) is the second smallest, only slightly higher than the value for cycle 15 (6.9). Clearly, values of *SM*, *Rm*, *Gm*, and *Am* now being experienced near cycle minimum for cycle 24 are near record values based on the reliable record of sunspot activity, not having been seen in about 100 yr.

Now, *SM*, *Gm*, and *Am* occurrences are closely associated with *Rm* occurrence. For example, based on cycles 10–23, 6 of 14 cycles had *SM* occurring simultaneously with *Rm*, and 12 of 14 cycles had *SM* occurring within 2 mo (either side) of *Rm*. The only exceptions were cycles 21 and 22, with *SM* leading *Rm* by 3 and 6 mo, respectively. Similarly, based on cycles 12–23, 7 of 12 cycles had *Gm* occurring simultaneously with *Rm*, and 9 of 12 cycles had *Gm* within 3 mo (either side) of *Rm*. The exceptions include cycles 13, 20, and 22, each leading *Rm* by 5, 4, and 6 mo, respectively. Finally, 9 of 12 cycles had *Am* occurring simultaneously with *Rm*, and 11 of 12 had *Am* occurring within 2 mo (either side) of *Rm*. The lone exception is cycle 21, which had *Am* lagging *Rm* by 5 mo. Presuming November 2008 to be cycle 24 minimum, all parameters appear to be reaching their extremes in value essentially simultaneously.

Figures 2 and 3 display the variation of the cyclic periods based on the parameters *SM*, *Rm*, *Gm*, and *Am*. As used here, period is defined as the elapsed time in months between successive occurrences of the parameters. Figure 2(a) shows the cyclic variation for the period using *SM* (i.e., *P*(*SM*–*SM*)), figure 2(b) shows the cyclic variation for the period using *Rm* (i.e., *P*(*Rm*–*Rm*)),

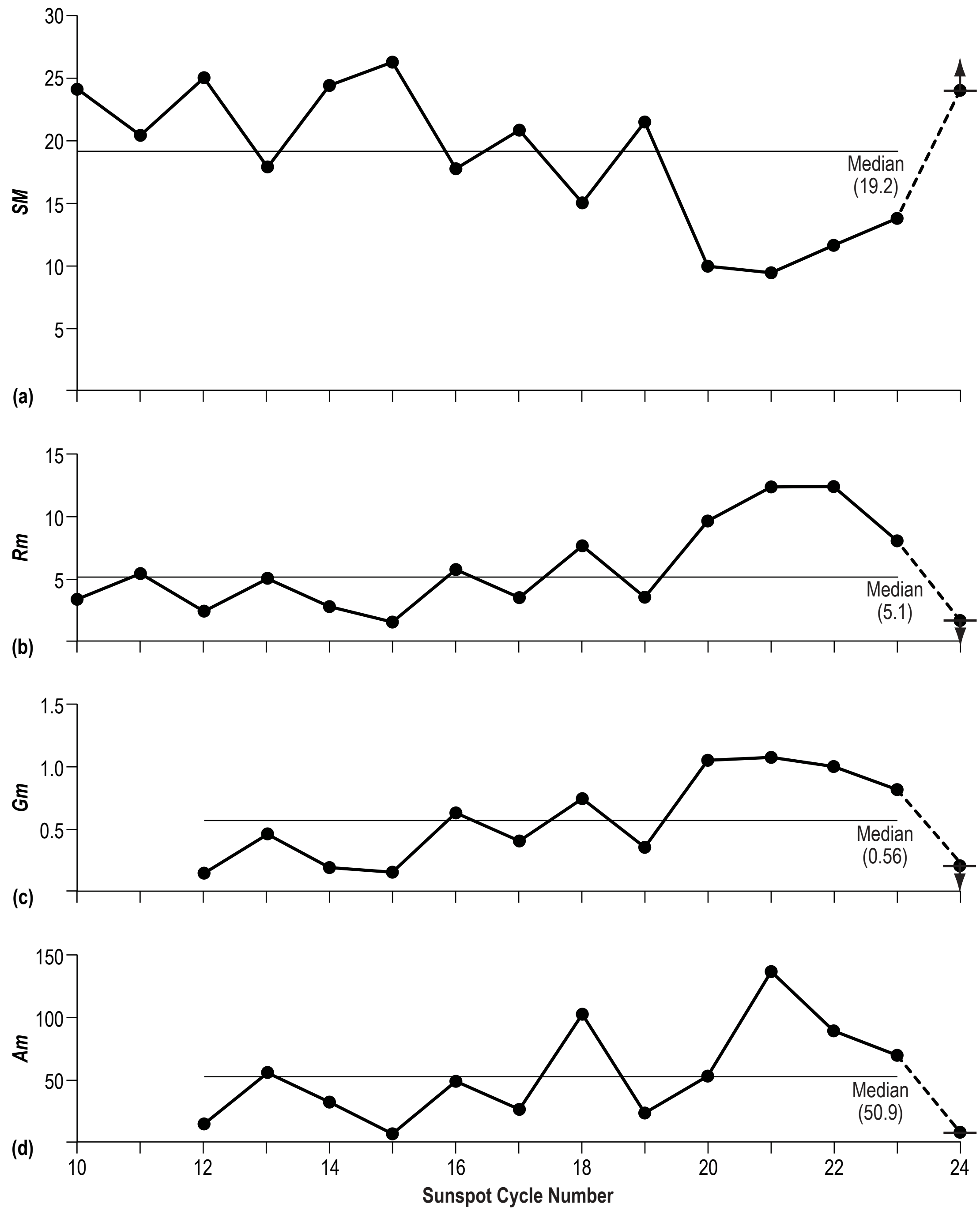

Figure 1. Cyclic variation of (a) *SM*, (b) *Rm*, (c) *Gm*, and (d) *Am* for cycles 10–24.

figure 3(a) shows the cyclic variation for the period using *Gm* (i.e., *P*(*Gm*–*Gm*)), and figure 3(b) shows the cyclic variation for the period using *Am* (i.e., *P*(*Am*–*Am*)). The horizontal line in each panel is the parametric mean. The dashed lines represent class extremes about the means, presuming the existence of two subgroupings— those cycles of shorter period than the mean and those of longer period than the mean. Wilson[13] previously has suggested that sunspot cycles can be grouped according to

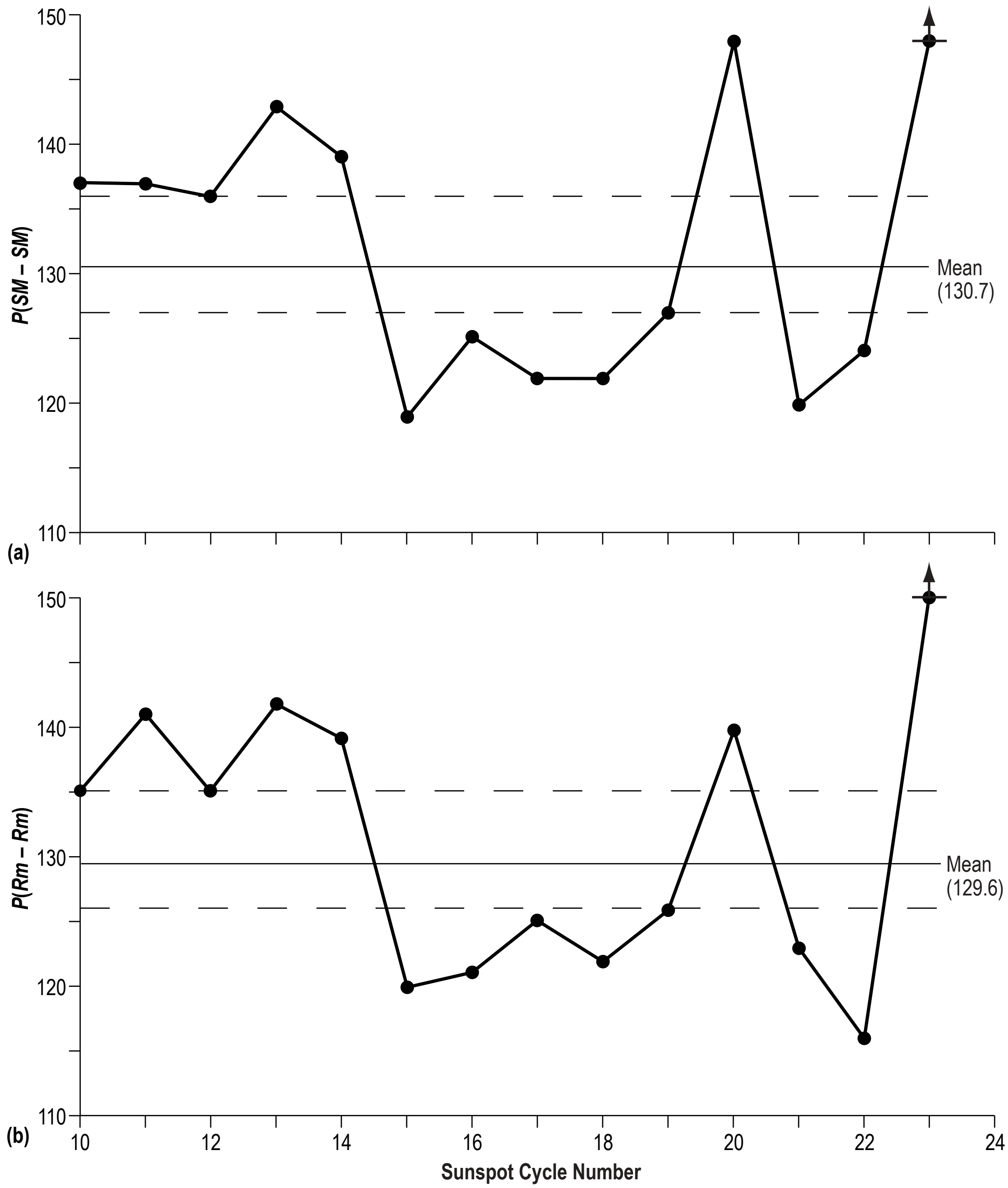

Figure 2. Cyclic variation of (a) *P*(*SM*–*SM*) and (b) *P*(*Rm*–*Rm*) for cycles 10–23.

period class when such cycles are described on the basis of 12-mma values, since the parametric mean clearly falls in the gap where no parametric values are found; i.e., there is no strong central clustering about the mean. Hence, while solar prognosticators often speak of an 11-yr average period for sunspot cycles, the record is better described as consisting of two classes of sunspot cycles: those of shorter period and those of longer period. (It should be noted, however, that using a longer smoothing function or a larger binning size negates the bimodal appearances as depicted here.)

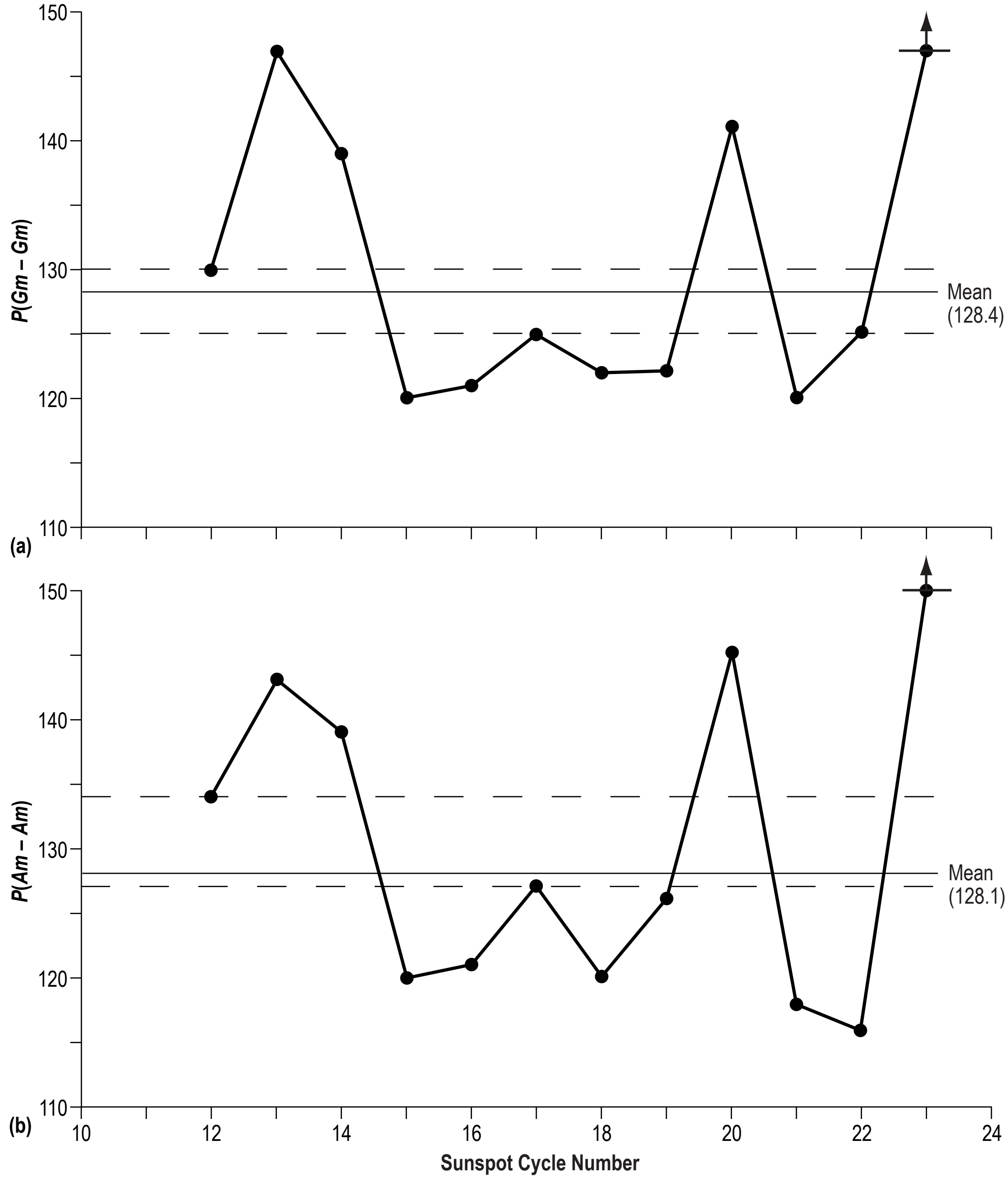

Figure 3. Cyclic variation of (a) $P(Gm–Gm)$ and (b) $P(Am–Am)$ for cycles 12–23.

For P(*SM–SM*) and P(*Rm–Rm*), cycles 10–14, 20, and now 23 are all cycles of longer duration, while cycles 15–19, 21, and 22 are all cycles of shorter duration. Compared to the mean *P*(*SM–SM*) using cycles 10–22 (130.7 mo), the tentative value (148 mo) for cycle 23's *P*(*SM–SM*) is about 1.8 standard deviations (*sd*) higher. Statistically speaking, there is only about a 5% chance that cycle 23's *P*(*SM–SM*) would extend 148 mo or more, inferring an epoch of *SM* date (*E*(*SM*)) for cycle 24 on or before November 2008 (i.e., 148 mo from July 1996, *E*(*SM*) for cycle 23), and there is only a 1% chance that P(*SM–SM*) would extend 158 mo or more, inferring *E*(*SM*) for cycle 24 on or before September 2009.

Compared to the mean $P(Rm–Rm)$ using cycles 10–22 (129.6 mo), the tentative value (150 mo) for cycle 23's $P(Rm–Rm)$ is about 2.2 *sd* higher. Only a 5% chance existed that cycle 23's $P(Rm–Rm)$ would extend 147 mo or more, which, clearly, it has already done, from cycle 23's epoch of *Rm* date ($E(Rm)$: May 1996). Only a 1% chance exists that cycle 23 would extend 155 mo or more, inferring $E(Rm)$ for cycle 24 on or before April 2009.

Compared to the mean $P(Gm–Gm)$ using cycles 12–22 (128.4 mo), the tentative value (147 mo) for cycle 23's $P(Gm–Gm)$ is about 1.9 *sd* higher. There is only about a 5% chance that cycle 23's $P(Gm–Gm)$ would extend 147 mo or more from cycle 23's epoch of *Gm* date ($E(Gm)$: August 1996), inferring $E(Gm)$ for cycle 24 to be on or before November 2008, and there is only a 1% chance that it would extend 156 mo or more, inferring $E(Gm)$ for cycle 24 on or before August 2009.

Last, compared to the mean $P(Am–Am)$ using cycles 12–22 (128.4 mo), the tentative value (147 mo) for cycle 23's $P(Am–Am)$ is about 2.1 *sd* higher. Again, there was only about a 5% chance that cycle 23's $P(Am–Am)$ would extend 148 mo or more from cycle 23's epoch of *Am* date ($E(Am)$: May 1996), inferring $E(Am)$ for cycle 24 to have been on or before September 2008, and there is only a 1% chance that it would extend 158 mo or more, inferring $E(Am)$ for cycle 24 on or before July 2009.

More recently, because new-cycle spots differentiate themselves from old-cycle spots by their magnetic configuration, where even-numbered sunspot cycles have positive leading polarity in the northern hemisphere (opposite in the southern hemisphere), and odd-numbered sunspot cycles have negative leading polarity in the northern hemisphere (opposite in the southern hemisphere), this characteristic is sometimes employed in the determination of sunspot minimum; i.e., the epoch date when the monthly number of new-cycle spots first dominates over old-cycle spots.[14] Unfortunately, because only recent cycles have sufficient magnetic configuration determinations to be used in the determination of new cycle spots, some other measure must serve as a proxy for new-cycle spots. An alternative to using the magnetic configuration for the determination of new-cycle spots might be one using the latitudinal distribution of sunspots near cycle minimum.

The latitudinal distribution of sunspots changes over the sunspot cycle. This was first noticed by Carrington in 1858 and confirmed first by Wolf (also in 1858) and later by Gustav Spörer (in 1867) and Father Pietro Angelo Secchi (in 1870).[2,5] The first spots of a new sunspot cycle usually begin appearing at latitudes above 25–30 deg N or S, and the last spots of the old sunspot cycle usually appear near the Sun's equator. The depiction of the resulting pattern of plotting the latitudinal position of sunspots against time takes on the appearance of butterfly wings; hence, the name 'butterfly diagram' is often used to describe it. Edward Walter Maunder was the first (in 1904) to show the full content and regularity of the pattern.[15]

Another way of depicting the latitudinal variation over a sunspot cycle is to fold the two hemispheres together.[16,17] As an example, figure 4(a) displays such a plot for the interval encompassing cycle 23 (January 1994–June 2009). The plot clearly shows the first occurrence of new-cycle, high-latitude spots in May 1996 for cycle 23 and the last old-cycle, low-latitude (near the equator) spots around April 1998 for cycle 22, suggesting an overlap of the two cycles of about 2 yr. It also clearly defines the latitudinal envelope of spots over the entire cycle. Noticeable is the expansion of the latitudinal distribution of spots as the cycle progresses from sunspot minimum to maximum and the flattening and declining of the upper envelope of the distribution especially after sunspot maximum, with the lowest latitude new-cycle spot (0 deg) first occurring in October 2000. The highest latitude new-cycle spot (50 deg) for cycle 23 occurred in early July 2001, slightly more than 1 yr past sunspot maximum (the spot was at 49 deg latitude in late June 2001), although one at 48 deg occurred in March 1998, about 2 yr prior to sunspot maximum.

Also shown are the variations of the 12-mma of the weighted mean latitude of sunspots: Figure 4(b) shows L, weighted by sunspot area, and figure 4(c) shows the highest latitude spot, H. The minimum and maximum values of L and H and their occurrence dates are identified. Figure 4(d) shows the variation of the ratio $g(h)/g$, where $g(h)$ is the monthly mean number of high-latitude groups (i.e., those having latitudes ≥25 deg) and g is the monthly mean number of all sunspot groups. Hence, the ratio identifies when new-cycle, high-latitude groups first become dominant contributors to solar activity (i.e., when $g(h)/g > 0.5$), which for cycle 23 occurred in June 1997, about 1 yr past sunspot minimum.

For cycle 23, which had Rm (8.0) in May 1996 and RM (120.8) in April 2000, Lm (7.8 deg) occurred in December 1995 and LM (23.1 deg) occurred in February 1998. Hm (16.1 deg) occurred in October 1995 and HM (38.4 deg) occurred in December 1999. As already mentioned, the ratio $g(h)/g$ was first greater than 0.5 in June 1997, and its peak (0.67) occurred in September 1997. Although a high-latitude (26-deg) spot was observed in March 1995, its magnetic configuration was that of old cycle 22 rather than new cycle 23. The first true new-cycle, high-latitude (38-deg) spot was seen in May 1996, occurring simultaneously with Rm. (The epoch of occurrence of $g(h)/g > 0.5$ varies markedly with respect to Rm. Five of 12 cycles have values preceding Rm by 2 to 8 mo, and 6 of 12 cycles have values lagging Rm by 3 to 13 mo. Only cycle 16 had a value occurring simultaneously with Rm. Presuming Rm in November 2008 for cycle 24, $g(h)/g > 0.5$ first preceded Rm by 2 mo.)

For cycle 24, Lm (6.6 deg) occurred in May 2007 and Hm (11.7 deg) occurred in June 2007. Rm has not, as yet, been officially discerned, although a value of R=1.8 was seen in November 2008, which is near record value (cycle 15 had an Rm=1.5 in August 1913). Values in November 2008 measured 16.0 deg for L and 20.8 deg for H. The ratio $g(h)/g$ was first greater than 0.5 in September 2008 and its peak (1.00) occurred in November and December 2008. Although a high-latitude (26-deg) spot was observed in October 2006, its magnetic configuration was that of old cycle 23 rather than new cycle 24. The first true new-cycle, high-latitude (30-deg) spot was observed in January 2008. (Previously, Wilson[18] used the first occurrence of a high-latitude spot to estimate the timing of cycle minimum.)

For comparison, figure 5 displays the 12-mma values for S (fig. 5(a)), R (fig. 5(b)), G (fig. 5(c)) and A (fig. 5(d)) for the interval January 1994–November 2008. For cycle 23, SM measured 13.8 in July 1996, occurring just 2 mo past Rm (8.0 in May 1996), and RM measured 120.8, occurring in April 2000. A slightly smaller secondary burst (R=115.5) of solar activity is observed to have peaked in November 2001, giving cycle 23 a double-humped appearance, such an appearance also being seen in cycles 20 and 22. The double-humped appearance is also found in G and A, although the later-occurring burst is the larger for these solar parameters. While smaller peaks in G and A occurred essentially simultaneously with RM, the true peaks in G and A followed RM, being

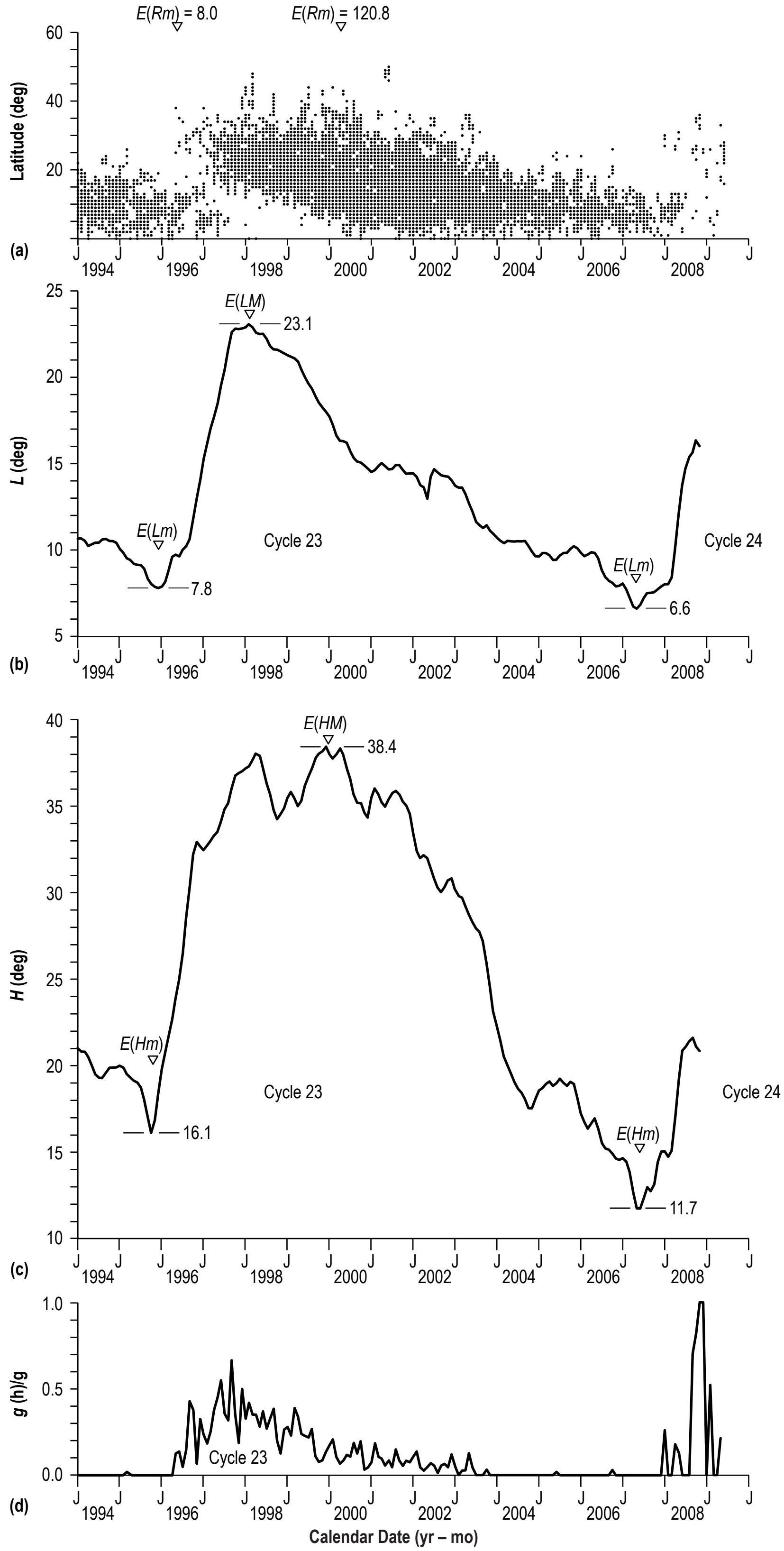

Figure 4. Monthly variation of (a) latitudinal distribution of spots, (b) L, (c) H, and (d) $g(h)/g$ for January 1994–November 2008.

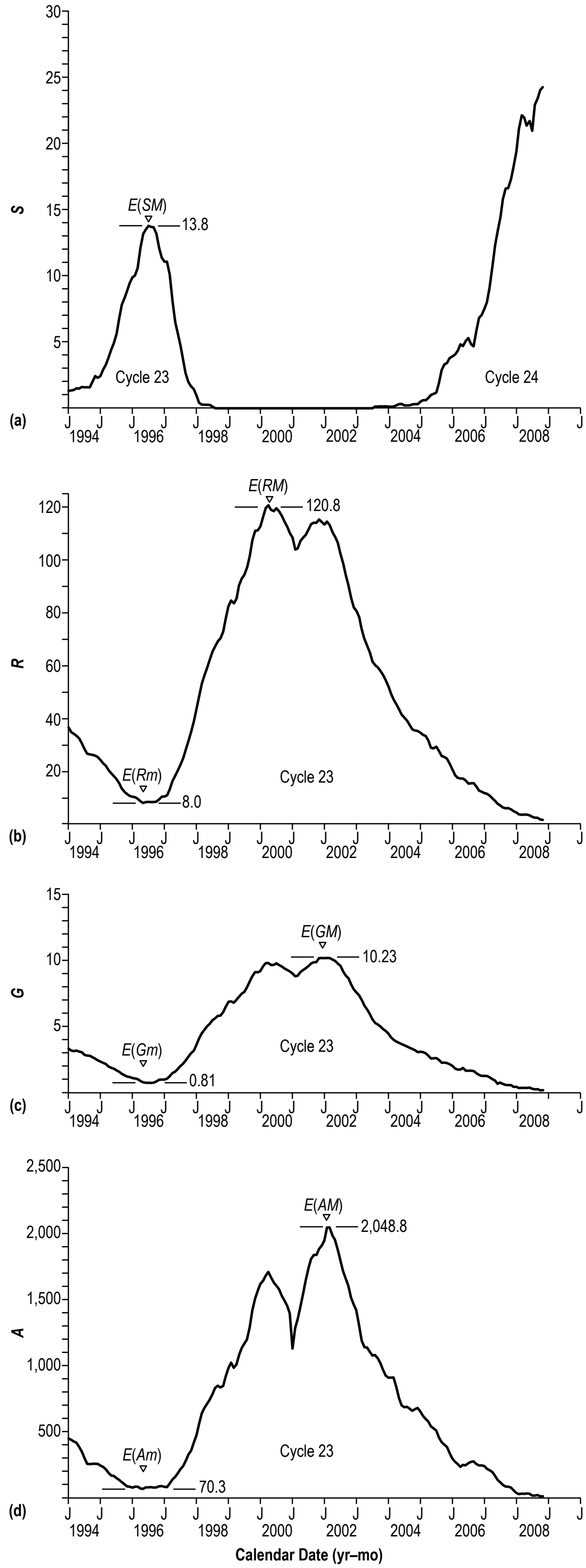

Figure 5. Monthly variation of (a) *S*, (b) *R*, (c) *G*, and (d) *A* for January 1994–November 2008,

associated with the secondary burst of activity in *R*. *GM* measured 10.23 in December 2001 and *AM* measured 2048.8 in February 2002. During the first peak, *G* measured 9.75 in March and April 2000, while *A* measured 1712.2 in April 2000. Thus, the secondary peak, which was about 5% smaller than *RM*, was about 5% larger as seen in *G* and 20% larger as seen in *A*.

Figure 6 plots the ratio of *A*/*G* for the same interval (January 1994–November 2008). Clearly, the area per group varied over cycle 23 by a factor greater than 3, from its minimum of 70.4 in February 1997 to 228.8 in March 2004. The values now being experienced (about 37.0) are below those seen in the mid-1990s, and, in fact, are lower than that seen in any previously observed cycle since cycle 12, dropping below the previous record held by cycle 15, which measured 46.0 in August 1913 (see fig. 7). Six of 12 cycles have (*A*/*G*)*m* occurring simultaneously with *Rm*, and 10 of 12 have (*A*/*G*)*m* occurring (either side) within 5 mo of *Rm*. The two exceptions are cycles 14 and 23, with lead and lag times of 23 and 9 mo, respectively. For cycle 24, *A*/*G* appears to be near minimum value in November 2008.

Figure 7 plots the minimum, maximum, and ratio values of *A*/*G* based on their 12-mma values for cycles 12–24, with cycle 24's values being considered tentative. Median values of 79.2 and 225.35 millionths of a visible solar hemisphere per group are found for (*A*/*G*)*m* and (*A*/*G*)*M*, respectively, for cycles 12–23. The ratio of (*A*/*G*)*M*/(*A*/*G*)*m* spans about 2.0 (cycle 13) to 4.1 (cycles 15 and 19) and has a median of 2.85. Correlation analysis (not shown) reveals only a marginally statistically significant (confidence level *cl* >90%) relationship between (*A*/*G*)*M* and (*A*/*G*)*m*.

Figure 8 plots the cyclic variation of *Lm* (fig. 8(a)), *LM* (fig. 8(b)), *Hm* (fig. 8(c)), and *HM* (fig. 8(d)). Also shown are the medians. While *Lm* and *LM* appear to show only slight variation with time (i.e., their values appear rather flat over time), in contrast, *Hm* and *HM* appear to have increased significantly in value between cycles 12 and 22, but now seem to be in decline. If this is true, then one expects cycle 24's *HM* to fall below the median (38.35 deg). Previously, Wilson and Hathaway[19] found a strong statistical relationship to exist between a cycle's maximum amplitude *RM* and *HM*, one that suggests cycle 24's *RM* to be below average size if its *HM* is below median value and larger than average size if its *HM* is above median value. Presently, *H* measures only about 21 deg, with *HM* not expected until late 2010 or later. (More will be said about the relationship between *RM* and *HM* in section 2.3.)

Figure 9 displays the elapsed time in months between the occurrences of *Lm* and *Rm* (*t*(*Lm*–*Rm*)) (fig. 9(a)) and between the occurrences of *Hm* and *Rm* (*t*(*Hm*–*Rm*)) (fig. 9(b)) for cycles 12–24. *Lm* and *Hm* have always preceded *Rm*, by 2–29 mo and 3–25 mo, respectively. The medians based on cycles 12–23 are 13 and 11.5 mo, respectively. Presuming November 2008 to be *E*(*Rm*) for cycle 24, its *Lm* and *Hm* both precede *E*(*Rm*) by 18 and 17 mo, respectively. For future sunspot cycles, including cycle 24's values, one anticipates that once *Lm* and *Hm* have been observed, *Rm* should be expected to follow within 6 to18 mo, having proved true for 7 of 13 cycles using *Lm* and 9 of 13 cycles using *Hm*.

Figure 10 shows the elapsed time in months between the occurrences of *Rm* and *LM* (*t*(*Rm*–*LM*)) (fig. 10(a)) and between the occurrences of *Rm* and *HM* (*t*(*Rm*–*HM*)) (fig. 10(b)) for cycles 12–23. *LM* and *HM* have always followed *Rm* by 4–24 and 14–52 mo, respectively. The medians are

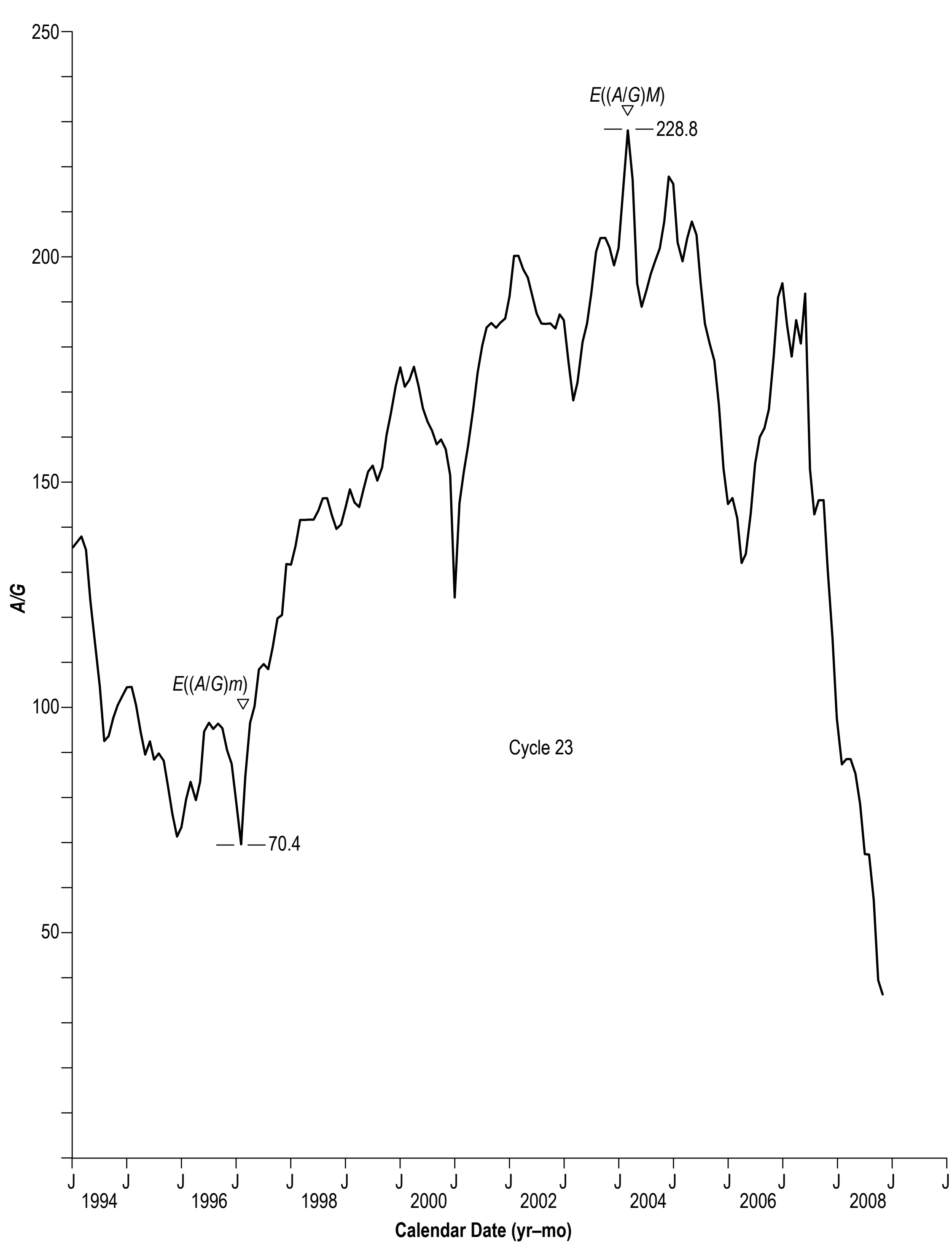

Figure 6. Monthly variation of A/G for January 1994–November 2008.

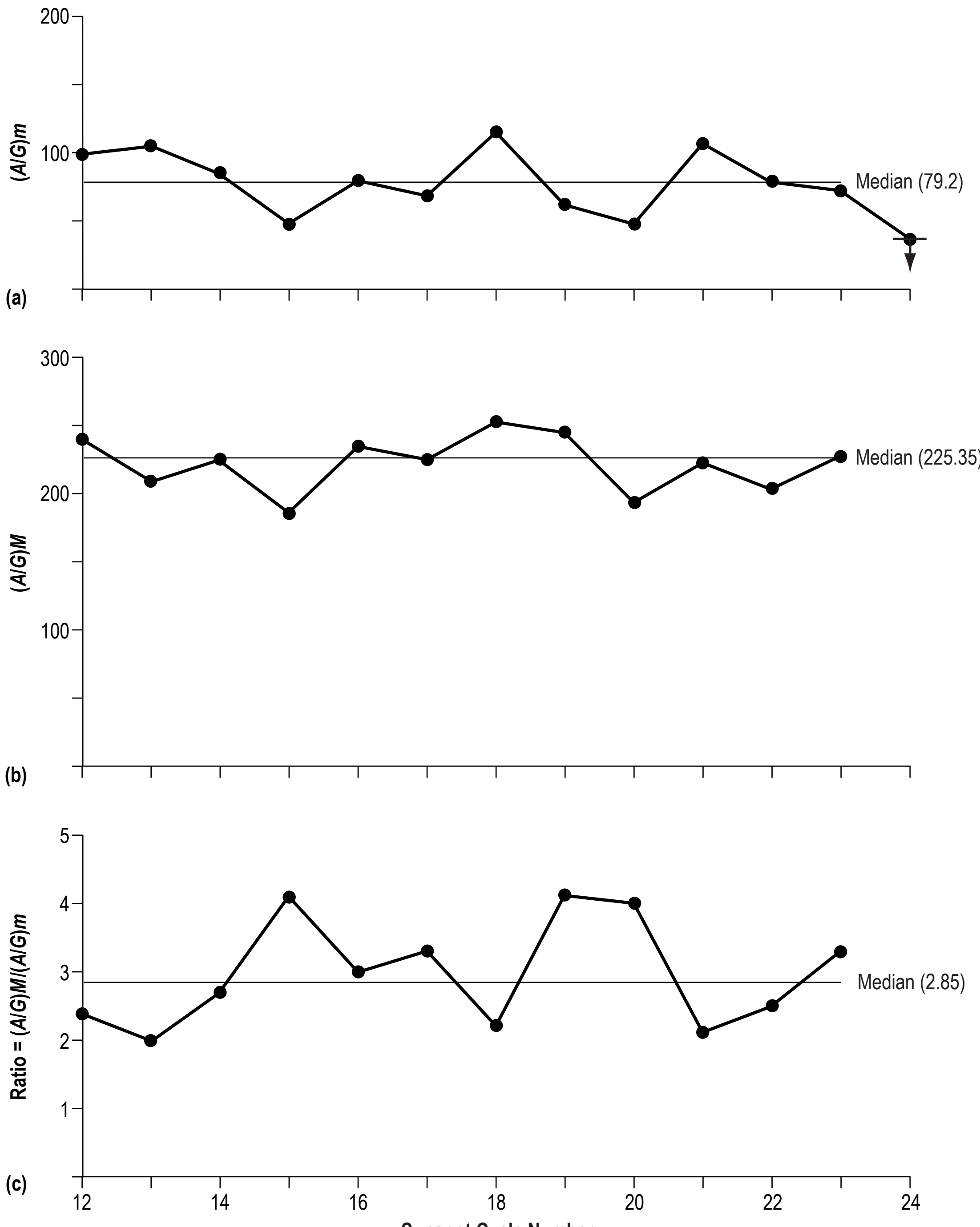

Figure 7. Cyclic variation of (a) $(A/G)m$, (b) $(A/G)M$, and (c) Ratio: $(A/G)M/(A/G)m$ for cycles 12–24.

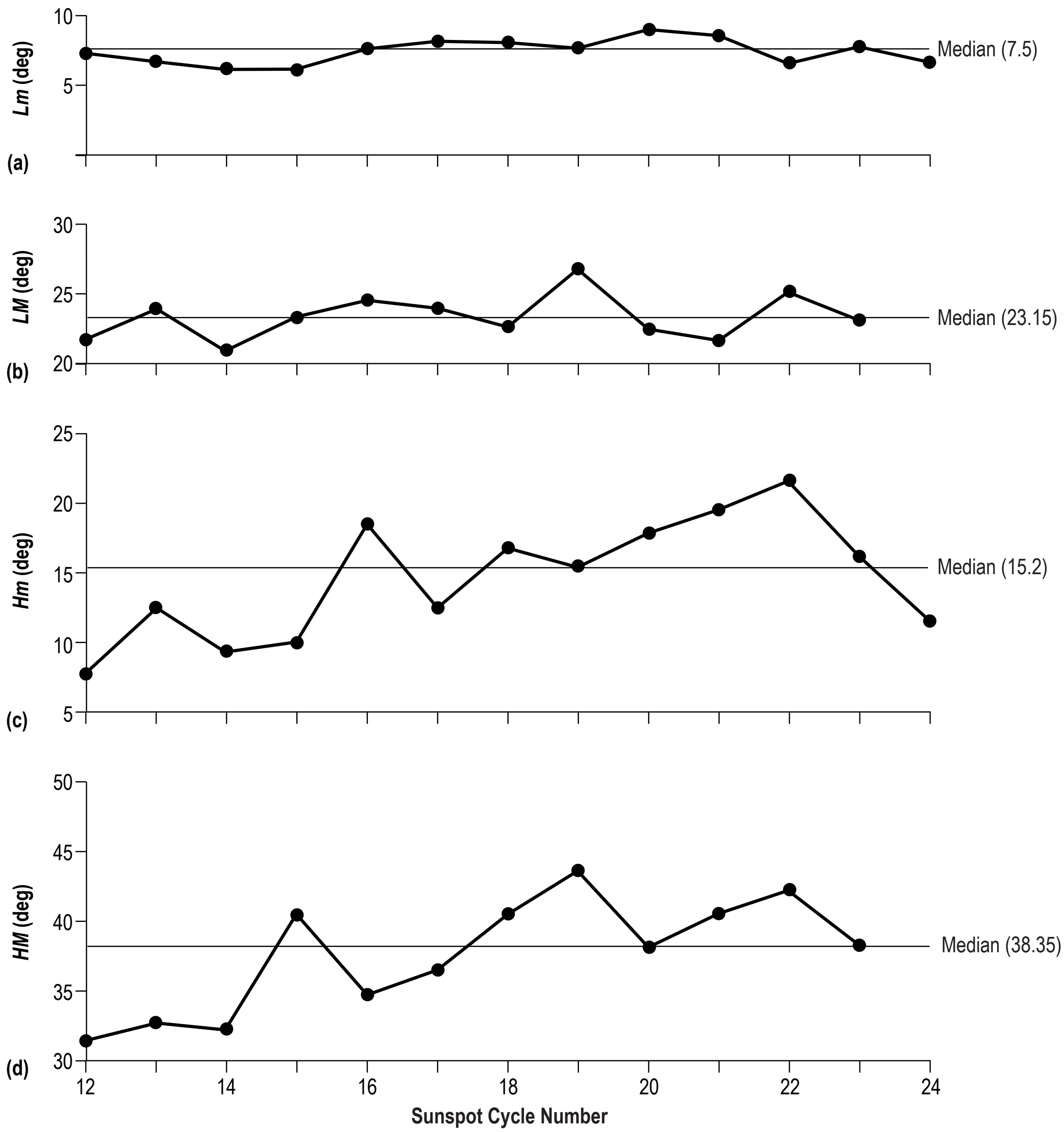

Figure 8. Cyclic variation of (a)*Lm*, (b) *LM*, (c) *Hm*, and (d) *HM* for cycles 12–24.

13 and 32 mo, respectively. For cycle 24, its *LM* is expected to follow November 2008 (presuming this to be *E*(*Rm*) for cycle 24) by about 8–15 mo, having proved true for 8 of 12 cycles, and HM is expected to follow by about 23–37 mo, having proved true for 8 of 12 cycles.

Figure 11 depicts the periods for each of the *L* and *H* parameters and when higher latitudes dominate ($g(h)/g > 0.5$): *P*(*Lm*–*Lm*) (fig. 11(a)), *P*(*LM*–*LM*) (fig. 11(b)), *P*(*Hm*–*Hm*) (fig. 11(c)), *P*(*HM*–*HM*) (fig. 11(d)), and *P*(0.5–0.5) (fig. 11(e)). Also shown are the means. Interestingly, the gap—delineated by the dashed lines—noticed in periods based on *S*, *R*, *G*, and *A* is also apparent in periods determined using *Lm* and *Hm*. Four of 5 cycles of longer than mean *P*(*Lm*–*Lm*)

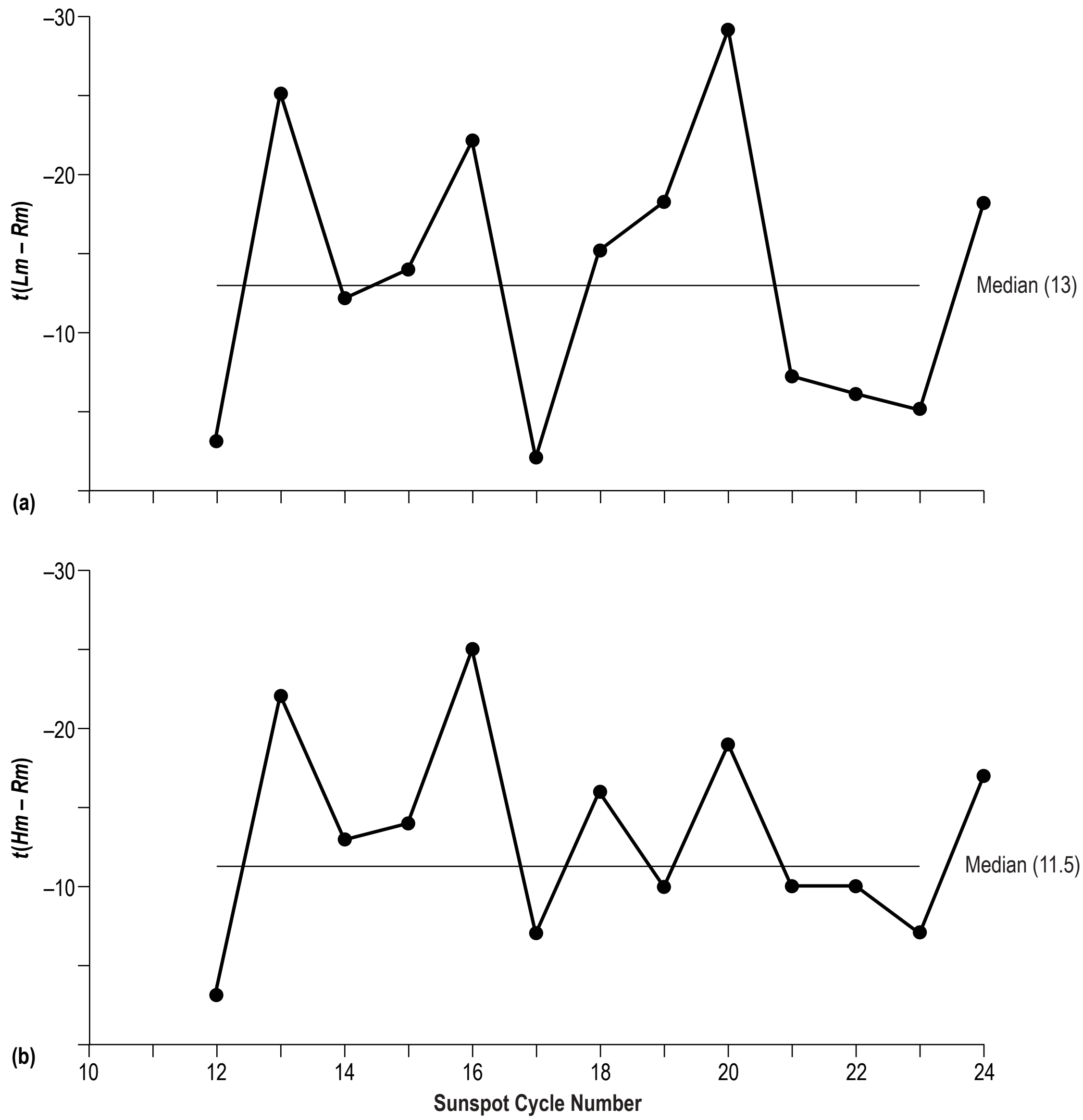

Figure 9. Cyclic variation of (a) $t(Lm–Rm)$ and (b) $t(Hm–Rm)$ for cycles 12–24.

or $P(Hm–Hm)$ (also $P(0.5–0.5)$) have longer periods as determined using S, R, G, and A. The only exception is cycle 16 (the exception is cycle 21 based on $P(0.5–0.5)$). Similarly, 6 of 7 cycles of shorter than mean $P(Lm–Lm)$ or $P(Hm–Hm)$ (also $P(0.5–0.5)$) have shorter periods as determined using S, R, G, and A; the only exception is cycle 12. Thus, because the epochs of Lm and Hm (not true for $E(g(h)/g > 0.5)$) precede minimum values of R, G, and A and maximum values of S, both $P(Lm–Lm)$ and $P(Hm–Hm)$ might be used to guess the period class for an ongoing sunspot cycle (i.e., a cycle of shorter or longer period), having proved correct for 10 of 12 sunspot cycles (7 of 7 cycles for cycles 17–23). For cycle 23, its $P(Lm–Lm)$ and $P(Hm–Hm)$ measured, respectively, 143 and 140 mo, suggesting cycle 23 to have $P(Rm–Rm)$ longer than the mean and longer than or equal to 135 mo, the lower extreme of longer period sunspot cycles based on R. This has proven correct since $P(Rm–Rm)$ for cycle 23 now measures at least 150 mo through October 2008, presuming $E(Rm)$ for cycle 24 in November 2008.

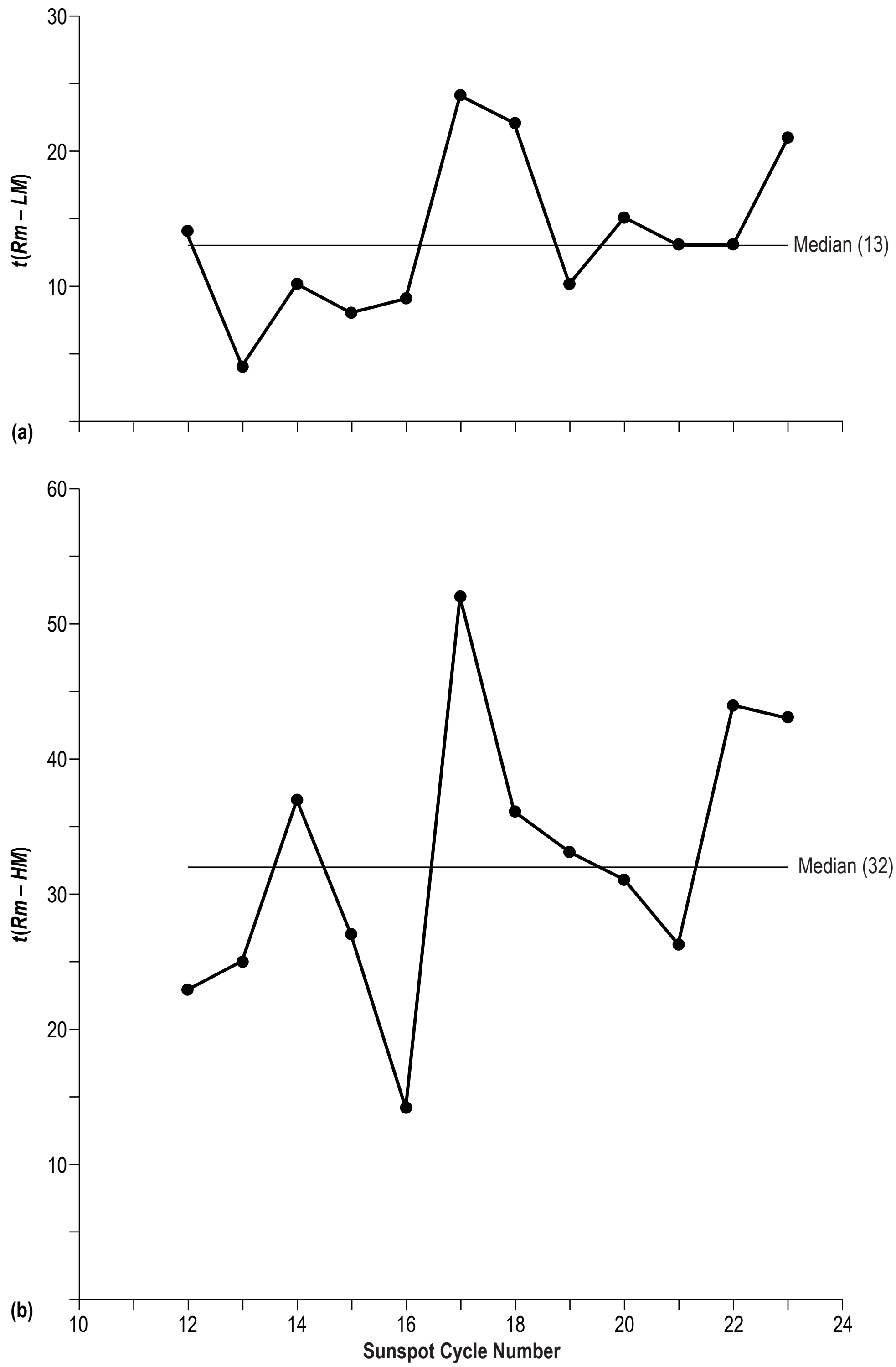

Figure 10. Cyclic variation of (a) $t(Rm–LM)$ and (b) $t(Rm–HM)$ for cycles 12–23.

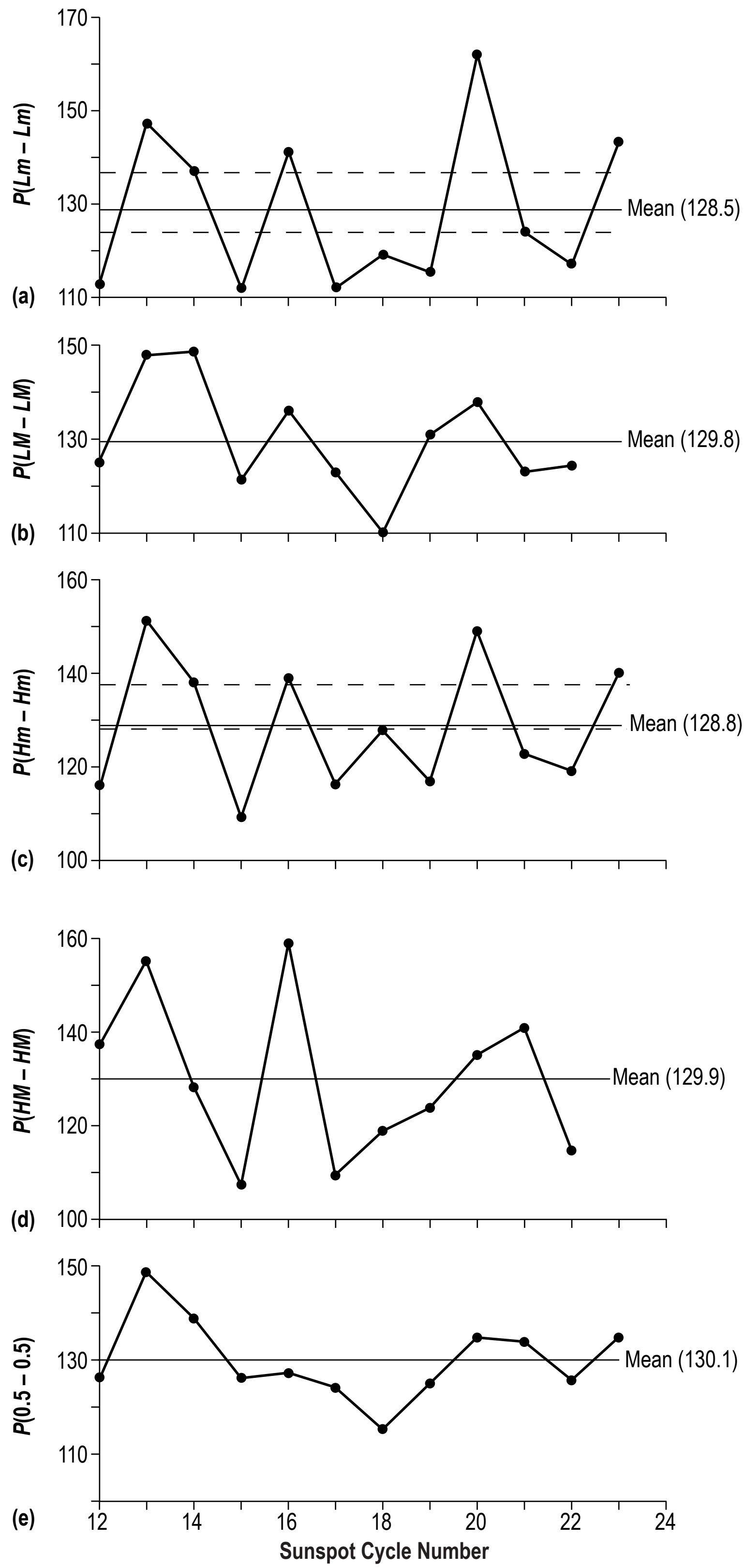

Figure 11. Cyclic variation of (a) $P(Lm–Lm)$, (b) $P(LM–LM)$, (c) $P(Hm–Hm)$, (d) $P(HM–HM)$, and (e) $P(0.5–0.5)$ for cycles 12–23.

For cycle 23, *LM* occurred in February 1998. Based on the median period for *LM* (about 130 mo), *LM* for cycle 24 should be expected about December 2008 (February 1998+130 mo). The value of *L* in November 2008, however, measures only 16.0 deg, well below all previous *LM* values. The lowest, 20.9 deg, occurred in November 1902 during cycle 14; see figure 8(b). The November 2008 value of *L* suggests, perhaps, that *LM* for cycle 24 still lies several months ahead. Because cycle 14 has the longest *P*(*LM*–*LM*), equal to 149 mo (fig. 11(b)), one infers that *LM* for cycle 24 probably should be expected within the next year, before July 2010. However, from figure 10(a), one expects *LM* to follow *Rm* by about 8–15 mo, suggesting *LM* will occur anytime between July 2010 and February 2011, which, if true, implies that *P*(*LM*–*LM*) for cycle 23 will be record setting (>149 mo).

Likewise, *HM* for cycle 23 occurred in December 1999. Based on the median period for *HM* (about 130 mo), *HM* for cycle 24 should be expected about October 2009. The value of *H* in November 2008 measured about 21 deg—again, far lower than all previous *HM* values (the lowest observed *HM* measured 31.5 deg during cycle 12; see fig. 8(d)). The shortest *P*(*HM*–*HM*) measures 107 mo (cycle 15; see fig. 11(d), inferring *HM* for cycle 24 on or after November 2008 (December 1999+ 107 mo). So, *HM* for cycle 24, likewise, appears to lie several months ahead, probably sometime before the end of 2010, although from figure 10(b), one expects *HM* to follow *Rm* by about 23–37 mo, suggesting HM would occur anytime between October 2010 and December 2011. If true, this suggests *P*(*HM*–HM) for cycle 23 would be about 130–144 mo.

Other periods of interest include those based on the elapsed time between the first spotless days (*FSD*) of successive cycles, the last spotless days (*LSD*) of successive cycles, and the first new-cycle, high-latitude spots (*FHLS*) of successive cycles, as well as the elapsed time between *FSD* and *Rm* and between *FHLS* and *Rm*. *FSD* is defined here as the first spotless day (i.e., when no spots are reported on the Sun as recorded by the Royal Observatory of Belgium, the caretakers of the International Sunspot Number) that occurs after the preceding cycle's *RM*. *LSD* is defined here as the last spotless day prior to the ongoing cycle's *RM*. Without magnetic configuration determinations, the first occurrence of the new cycle's *FHLS* is inherently speculative. Here, however, *FHLS* is taken to be the first occurrence of a high-latitude spot (≥25 deg latitude) during the decline of the cycle, within the last 3 yr of the cycle, and always either before or simultaneous with *Rm* occurrence, especially after a lengthy continuous run of lower-latitude spot occurrences. Using the folded hemispheric representation of the latitudinal distribution of sunspots facilitates the selection of *FHLS*, as shown in figure 12 for cycles 12–24, plotted relative to *Rm* occurrence. For cycle 24, its tentative representation presumes *Rm* occurrence in November 2008.

Figure 12 shows the latitudinal distribution of sunspots within 3 yr prior to sunspot minimum through 2 yr post sunspot minimum for cycles 12–24. Notice that all cycles have *FHLS* either prior to or simultaneously with *Rm* occurrence. Notice also that the overlap of old and new cycles tends to be about 1–4 yr, i.e., the elapsed time from *FHLS* of the new cycle to the last lowest-latitude spot (*LLLS*) of the old cycle near the equator. While the actual *FHLS*s for cycles 21 and 22 seem somewhat ambiguous (i.e., the occurrences might be slightly closer to their *E*(*Rm*) dates), for the remainder of the cycles *FHLS* appears well determined.

Figure 13 depicts the cyclic variation of the elapsed time in months from *FHLS* to *LLLS* (i.e., *t*(*FHLS*–*LLLS*)) individually for cycles 12–23, with tentative values shown for cycle 23 (>157 mo,

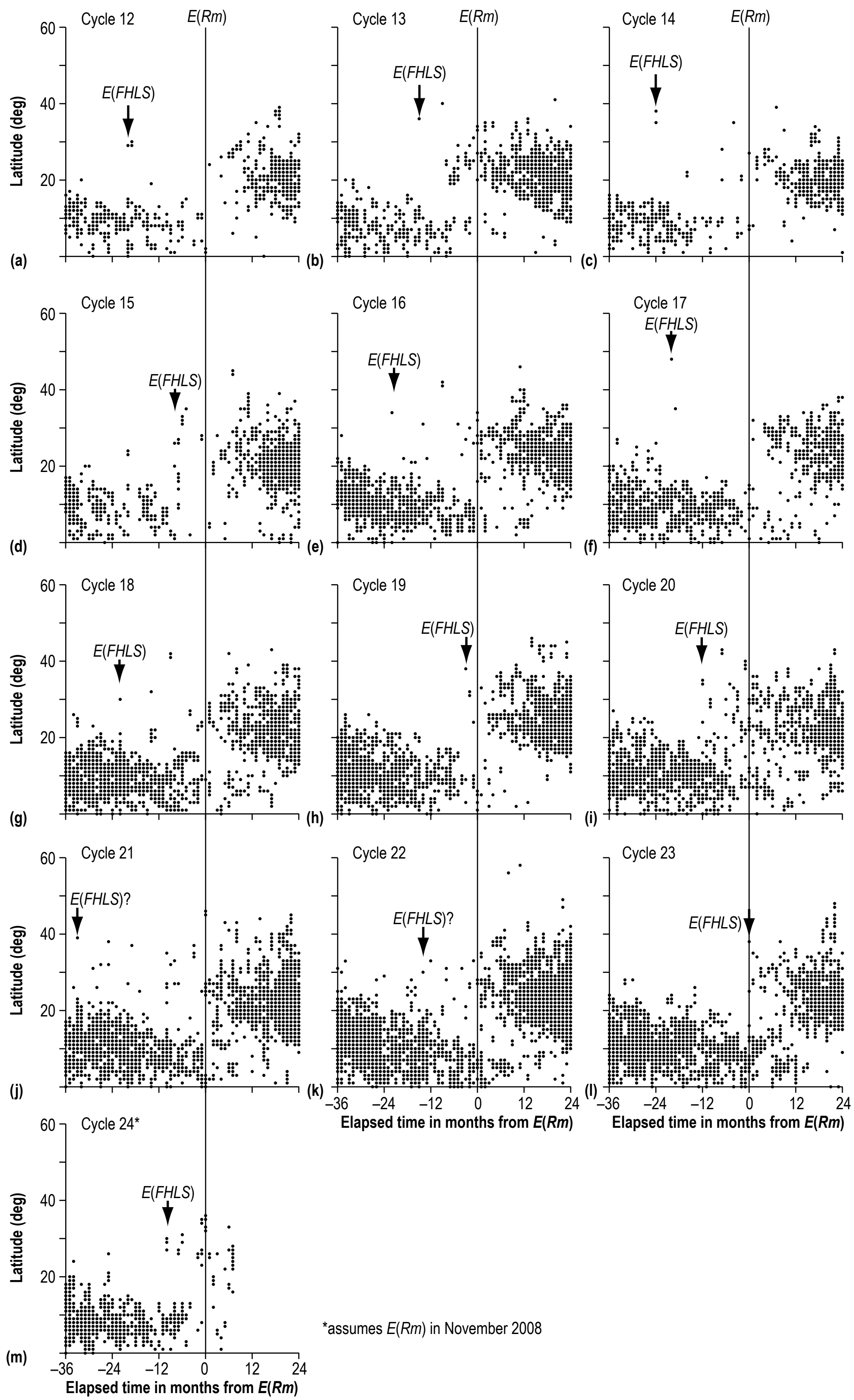

Figure 12. Cycle-by-cycle latitudinal distribution of spots for cycles 12–24 for elapsed time in months from 36 mo prior to $E(Rm)$ to 24 mo after $E(Rm)$.

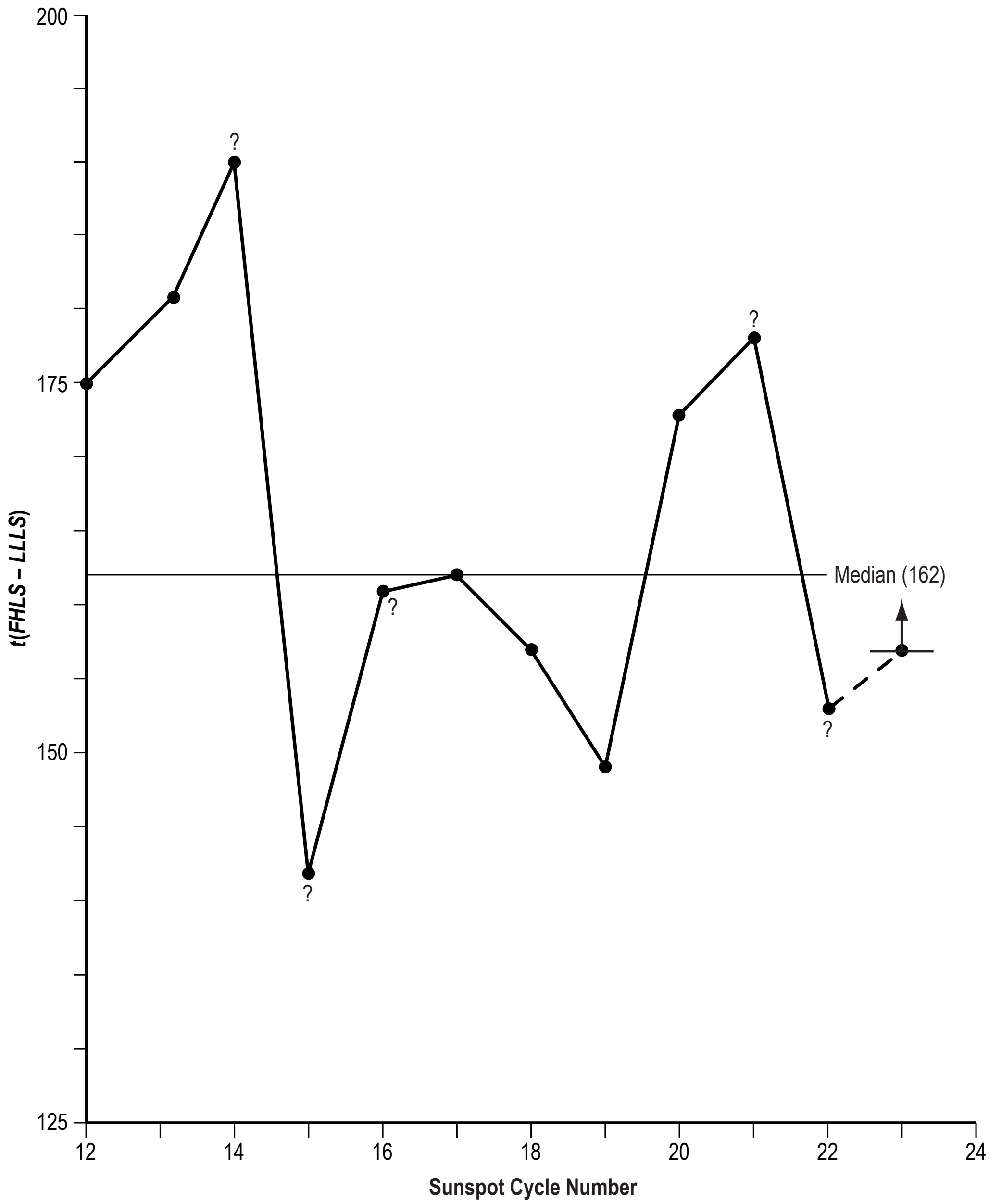

Figure 13. Cyclic variation of *t*(*FHLS*–*LLLS*) for cycles 12–23.

through June 2009) and those of questionable length identified using question marks. The median is 162 mo (about 13.5 yr), and the range is 142 mo (cycle 15) to 190 mo (cycle 14). Interestingly, for every cycle, *t*(*FHLS*–*LLLS*) is longer than its corresponding *P*(*Rm*–*Rm*), averaging about 37 mo longer (range: 22–55 mo). This suggests that *LLLS* for cycle 23 probably remains well in the future, since the difference between the presumed *E*(*Rm*) for cycle 24 (November 2008) and June 2009 is only 7 mo. The epoch of *LLLS* for cycle 23 seems likely not to occur until after about September 2010, unless cycle 23 proves to be a statistical outlier. Also interesting is that 4 of 5 cycles with *t*(*FHLS*–*LLLS*) ≥173 mo are longer-period sunspot cycles (the exception is cycle 21), and 6 of 7 cycles with *t*(*FHLS*–*LLLS*) ≤162 mo are shorter-period cycles (the exception is cycle 23, having *t*(*FHLS*–*LLLS*) >157 mo).

Figure 14 plots the variation of the elapsed time in months from the occurrence of *FHLS* to *Rm* for cycles 12–24 (*t*(*FHLS*–*Rm*)), where cycle 24's elapsed time presumes *Rm* occurrence in November 2008. Because the occurrences for *FHLS* for cycles 21 and 22 are somewhat uncertain, for these two cycles the elapsed time could be slightly shorter (hence, the use of question marks for their *t*(*FHLS*–*Rm*) values). The median is –14.5 mo and, including cycle 24, 5 of the past 6 cycles have had *t*(*FHLS*–*Rm*) values shorter than the median. All of the cycles have had *FHLS* occurrence within 2 yr (leading) of *Rm* occurrence, except, possibly, cycle 21. (Presuming *Rm* in November 2008 for cycle 24, *t*(*FHLS*–*Rm*) equals –10 mo.)

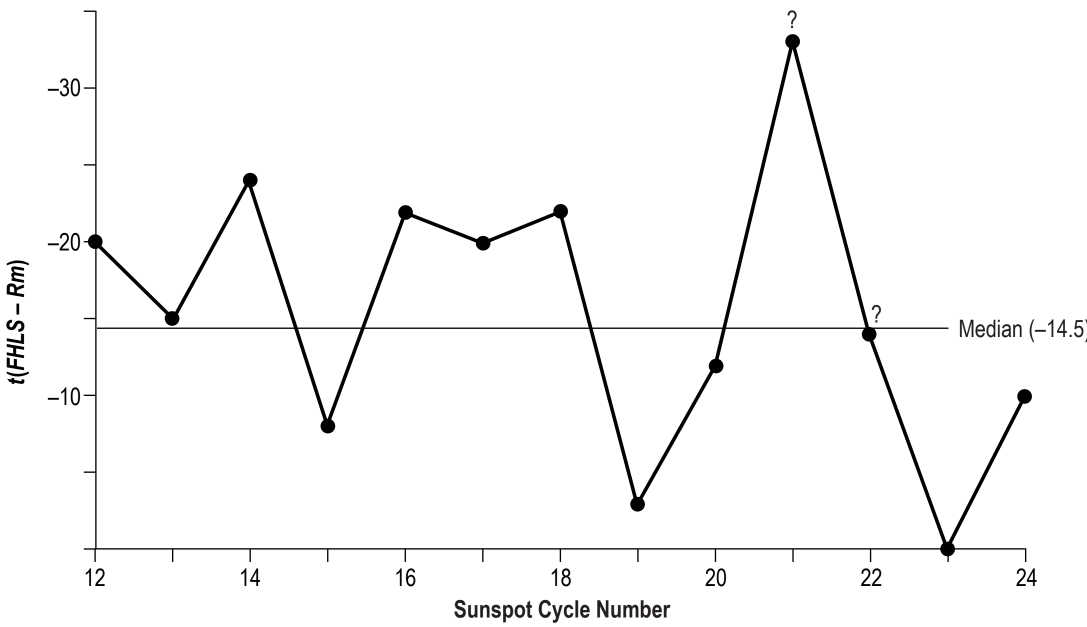

Figure 14. Cyclic variation of *t*(*FHLS*–*Rm*) for cycles 12–24.

Figure 15 plots the variation of the periods based on *FSD* and *LSD*: *P*(*FSD*–*FSD*) in figure 15(a) and P(*LSD*–*LSD*) in figure 15(b). For *P*(*FSD*–*FSD*), its mean is about 132 mo with the hint of a downward trend between cycles 12 and 23 and with 5 of the past 6 cycles having *P*(*FSD*–*FSD*) below the mean value. If the trend continues, then *FSD* for cycle 25 should occur before January 2015 (January 2004+132 mo). For *P*(*LSD*–*LSD*), its mean is about 129 mo, so one infers *LSD* for cycle 23 about October 2008, which has already passed. Spotless days continue to be seen in the overlap of cycles 23 and 24 (through July 2009), so one infers *t*(*LSD*–*LSD*) for cycle 23 >138 mo. Cycle 23's *t*(*LSD*–*LSD*) is now the third longest ever seen, although still far shorter than that seen for cycles 13 (170 mo) and 15 (163 mo). Should cycle 23 be closely akin to these cycles, spotless days might continue to be seen during cycle 24 for another 2–3 yr.

Figure 16 displays the variation of the leading elapsed time between *FSD* and *Rm* occurrences (*t*(*FSD*–*Rm*), fig. 16(a)), the lagging elapsed time between *Rm* and *LSD* occurrences (*t*(*Rm*–*LSD*), fig. 16(b)), and the elapsed time between *FSD* and *LSD* occurrences (*t*(*FSD*–*LSD*), fig. 16(c)) for cycles 10–24. Concerning *t*(*FSD*–*Rm*), prior to cycle 24, its value was –62 mo or more for

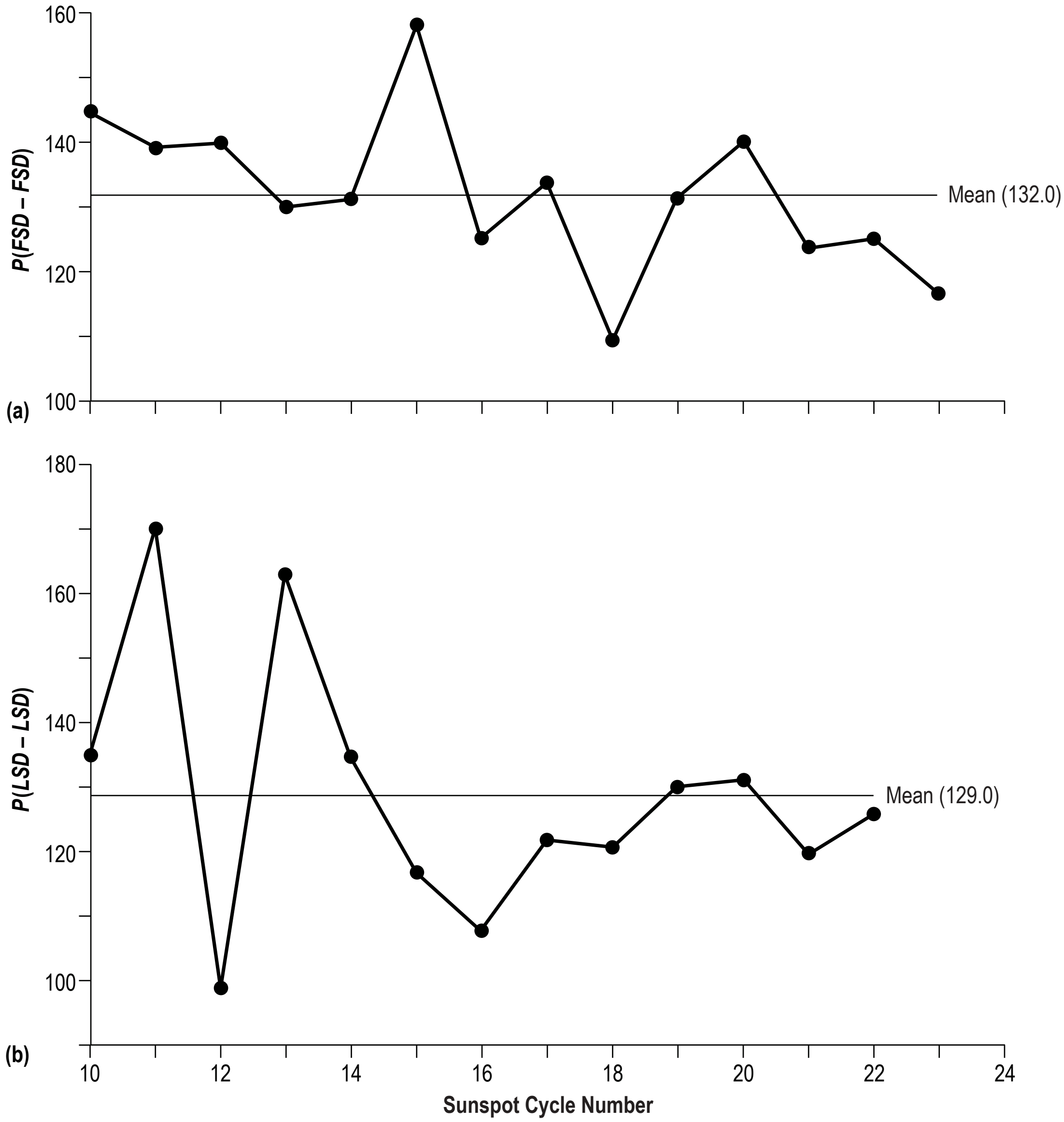

Figure 15. Cyclic variation of (a) *P*(*FSD*–*FSD*) and (b) *P*(*LSD*–*LSD*) for cycles 10–23.

cycles 10–15 and –40 mo or less for cycles 16–23; i.e., a large gap is perceived between the earlier cycles and the more recent cycles. Presuming *Rm* occurrence for cycle 24 to be November 2008, its *t*(*FSD*–*Rm*) measures –58 mo, a value more akin to the earlier cycles than the more recent cycles, but 4 mo shorter than the upper extreme of the perceived gap. Could cycle 24 be the start of another extended interval of *t*(*FSD*–*Rm*) measuring about 5 yr or longer?

Concerning *t*(*Rm*–*LSD*), 7 of the past 7 cycles have had values below the mean (26.5 mo). So, if cycle 24's *Rm* occurrence is indeed November 2008, then *LSD* for cycle 24 should occur before February 2011 and probably before May 2010, based on the average length for the past 7 cycles. Through July 2009, *t*(*Rm*–*LSD*) measured 8 mo, a value below the 10 mo observed for cycle 22, so spotless days should continue at least another 2 mo and probably longer; i.e., *LSD* for cycle 24 should not be expected before September 2009, based on the recent behavior of *t*(*Rm*–*LSD*).

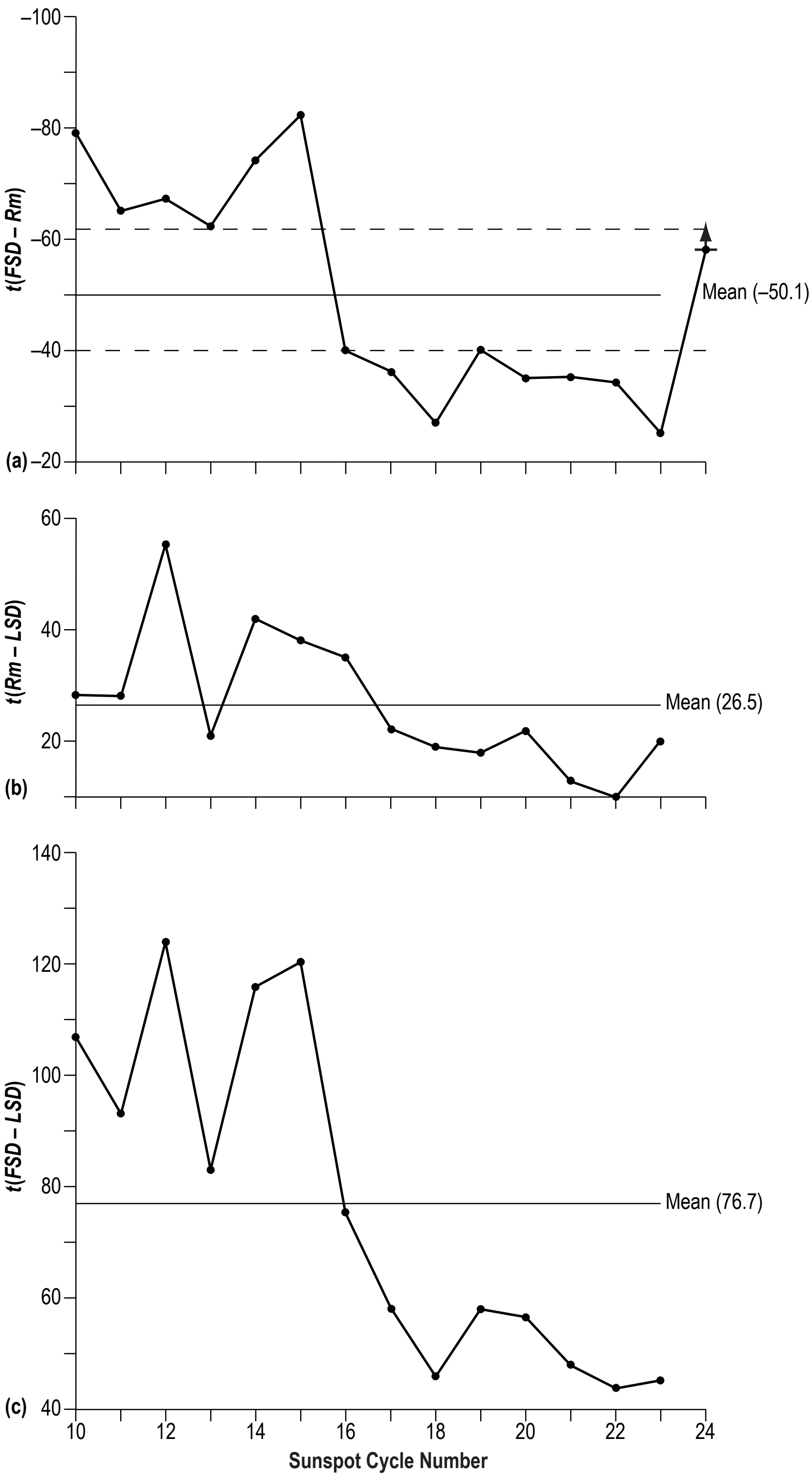

Figure 16. Cyclic variation of (a) $t(FSD–Rm)$, (b) $t(Rm–LSD)$, and (c) $t(FSD–LSD)$ for cycles 10–24.

Concerning t(*FSD–LSD*), it too has behavioral traits suggestive of characteristic differences between the earlier cycles 10–15 and the more recent cycles 16–23. Cycles 10–15 have t(*FSD–LSD*) longer than the mean (about 77 mo), while cycles 16–23 have t(*FSD–LSD*) shorter than the mean. In fact, 7 of the past 7 cycles have values averaging only about 51 mo, ranging between 44 and 58 mo. Hence, if cycle 24 is akin to the more recent cycles, then the length of time in months from *FSD* to *LSD* should be less than 77 mo, implying *LSD* for cycle 24 before June 2010 (January 2004+ 77 mo). Presently, spotless days have been observed for 66 mo, so, presuming cycle 24 to be more akin to recent cycles, a rapid transition to fewer spotless days should now be underway, with *LSD* for cycle 24 expected within 12 mo. However, if cycle 24 is more akin to the earlier cycles, as suggested by t(*FSD–Rm*), then *LSD* for cycle 24 will be delayed until after June 2010, more likely after about December 2010, and possibly as late as December 2012, based on the average length of t(*FSD–LSD*) for cycles 10–15, which measures about 107 mo. (Wilson[20] and Wilson and Hathaway[21–23] have provided additional material concerning spotless days and their relationship to the sunspot cycle and the prediction of sunspot minimum.)

For convenience, included here are tables 1–4, which identify, respectively, the various epochs of occurrence for the selected solar cyclic parameters, the values for the selected solar cyclic parameters, the periods for the selected solar cyclic parameters, and the elapsed times relative to *E*(*Rm*) for the selected solar cyclic parameters.

2.2 Parametric Variations Near Cycle Maximum

Figure 17 plots the cyclic variation of *RM* (fig. 17(a)), *GM* (fig. 17(b)), and *AM* (fig. 17(c)) for cycles 10–23. The medians are 114.9, 9.9, and 1,834.1, respectively. Cycle 23 had values just above the medians. For each parameter, correlation analysis suggests a statistically significant rise (secular variation) during the observed intervals, given by the diagonal lines. Presuming the inferred trend continues, cycle 24 is expected to have RM=158.1 ± 34.5 (± 1σ accuracy), GM=14.2 ± 2.3 (± 1σ accuracy), and AM=2,769.7 ± 598.1 (± 1σ accuracy). However, if the trends are now downward, possibly having peaked about cycle 19, then one expects values for the parameters to fall below the medians. (Wilson[24] and Hathaway, Wilson, and Reichmann[12] have previously drawn attention to the secular rise in sunspot number.)

Figure 18 shows the periods associated with each of the parameters: *P*(*RM–RM*) (fig. 18(a)), *P*(*GM–GM*) (fig. 18(b)), and *P*(*AM–AM*) (fig. 18(c)). The medians are 128, 127, and 126 mo, respectively. Eight of 13 cycles have *P*(*RM–RM*)=128 ± 6 mo, with 2 of the past 3 cycles falling within the bounds, suggesting cycle 24's *RM* would occur about December 2010 (±6 mo), given *E*(*RM*) of April 2000 for cycle 23. However, this seems far too early, given that *E*(*Rm*) for cycle 24 has only just occurred (about November 2008). To accept *P*(*RM–RM*)=128 ± 6 mo implies a very fast rise for cycle 24, one measuring just 25 ± 6 mo, which is shorter than ever seen. The fastest rise to date (34 mo) was observed for cycle 22, the third largest cycle on record (*RM*=158.5). A more modest rise of 48 mo gives *E*(*RM*) for cycle 24 about November 2012 and yields *P*(*RM–RM*)=151 mo, which would make it the second longest *P*(*RM–RM*) on record, slightly shorter than observed for cycle 11's *P*(*RM–RM*).

Table 1. Epochs of occurrence for selected solar cyclic parameters.

Cycle	E(Rm)	E(SM)	E(Gm)	E(Am)	E(g(h)/g >0.5)	E(Lm)	E(Hm)	E(RM)	E(GM)	E(AM)	E(LM)	E(HM)	E(FSD)	E(LSD)	E(FHLS)	E(LLLS)	E((A/G)m)	E((A/G)M)
10	12–1855	12–1855	–	–	–		02–1860	–	–	–	–	05–1849	04–1858	–	–	–	–	
11	03–1867	05–1867	–	–	–		08–1870	–	–	–	–	10–1861	07–1869	–	03–1880	–	–	
12	12–1878	10–1878	12–1878	12–1878	06–1879	09–1878	09–1878	12–1883	03–1884	11–1883	02–1880	11–1880	05–1873	09–1883	04–1877	11–1891	07–1878	03–1883
13	03–1890	02–1890	10–1889	02–1890	12–1889	02–1888	05–1888	01–1894	09–1893	01–1894	07–1890	04–1892	01–1885	12–1891	12–1888	01–1904	03–1890	02–1897
14	01–1902	01–1902	01–1902	01–1902	05–1902	01–1901	12–1900	02–1906	02–1906	06–1905	11–1902	03–1905	11–1895	07–1905	01–1900	11–1915?	02–1900	06–1905
15	08–1913	08–1913	08–1913	08–1913	02–1913	06–1912	06–1912	08–1917	07–1917	08–1917	04–1914	11–1915	10–1906	10–1916	12–1912	10–1924?	08–1913	10–1921
16	08–1923	10–1923	08–1923	08–1923	08–1923	10–1921	07–1921	04–1928	06–1928	06–1928	05–1924	10–1924	04–1920	07–1926	10–1921	03–1935?	08–1923	04–1926
17	09–1933	09–1933	09–1933	09–1933	03–1934	07–1933	02–1933	04–1937	04–1937	05–1937	09–1935	01–1938	09–1930	07–1935	01–1932	07–1945	09–1933	07–1943
18	02–1944	02–1944	02–1944	04–1944	07–1944	11–1942	10–1942	05–1947	11–1947	05–1947	12–1945	02–1947	11–1941	09–1945	04–1942	05–1955	05–1944	12–1946
19	04–1954	04–1954	04–1954	04–1954	02–1954	10–1952	06–1953	03–1958	03–1958	11–1957	02–1955	01–1957	12–1950	10–1955	01–1954	06–1966	05–1954	10–1957
20	10–1964	11–1964	06–1964	10–1964	07–1964	05–1962	03–1963	11–1968	06–1970	04–1968	01–1966	05–1967	11–1961	08–1966	10–1963	03–1978	10–1964	06–1968
21	06–1976	03–1976	03–1976	11–1976	10–1975	11–1975	08–1975	12–1979	06–1979	10–1981	07–1977	08–1978	07–1973	07–1977	09–1973?	07–1988	11–1976	01–1982
22	09–1986	03–1986	03–1986	09–1986	12–1986	03–1986	11–1985	07–1989	02–1991	05–1989	10–1987	05–1990	11–1983	07–1987	07–1985?	04–1998	09–1986	05–1989
23	05–1996	07–1996	08–1996	05–1996	06–1997	12–1995	10–1995	04–2000	12–2001	02–2002	02–1998	12–1999	04–1994	01–1998	05–1996*	–	02–1997	03–2004
24	(11–2008)	(11–2008)	(11–2008)	(11–2008)	09–2008	05–2007	06–2007	–	–	–	–	–	01–2004	–	01–2008*	–	11–2008?	

* based on actual magnetic configuration

Table 2. Values of selected solar cyclic parameters.

Cycle	*Rm*	*SM*	*Gm*	*Am*	*Lm*	*Hm*	*RM*	*GM*	*AM*	*LM*	*HM*	*FHLS*	*(A/G)m*	*(A/G)M*
10	3.2	24.1	–	–	–	–	97.9	–	–	–	–	–	–	–
11	5.2	20.4	–	–	–	–	140.5	–	–	–	–	–	–	–
12	2.2	25.0	0.15	15.1	7.3	7.8	74.6	6.29	1,406.6	21.8	31.5	28.6	98.6	240.2
13	5.0	17.9	0.48	56.5	6.6	12.6	87.9	8.66	1,610.6	24.0	32.8	35.5	103.3	209.3
14	2.6	24.3	0.20	31.7	6.1	9.4	64.2	5.74	1,192.3	20.9	32.2	38.4	83.7	225.4
15	1.5	26.2	0.15	6.9	6.1	9.9	105.4	9.58	1,570.9	23.2	40.5	26.3	46.0	186.7
16	5.6	17.8	0.63	49.8	7.6	18.5	78.1	7.07	1,369.9	24.4	34.8	34.0?	79.0	234.5
17	3.4	20.8	0.41	27.7	8.0	12.5	119.2	10.69	2,160.1	24.0	36.5	48.0	67.6	225.3
18	7.7	15.0	0.74	101.8	8.0	16.8	151.8	11.85	2,713.5	22.7	40.5	30.3	116.1	251.1
19	3.4	21.4	0.36	23.5	7.5	15.2	201.3	14.82	3,547.7	26.9	43.6	37.8	60.5	246.3
20	9.6	9.9	1.05	51.9	8.9	17.9	110.6	9.33	1,619.3	22.3	38.3	35.0	48.1	192.4
21	12.2	9.4	1.09	138.2	8.4	19.6	164.5	14.88	2,524.6	21.7	40.5	35.4?	106.3	223.4
22	12.3	11.7	1.00	88.9	6.5	21.7	158.5	13.57	2,592.7	25.2	42.4	30?	79.4	202.2
23	8.0	13.8	0.81	70.3	7.8	16.1	120.8	10.23	2,048.8	23.1	38.4	38	70.4	228.8
24	(1.8)	(24.2)	(0.20)	(7.4)	6.6	11.7	–	–	–	–	–	30	(37.0)	–

Regarding $P(GM–GM)$, 6 of 11 cycles have $P(GM–GM)=127 \pm 6$ mo, with 2 of the past 3 cycles falling within the bounds, implying cycle 24's GM would occur about July 2012 (±6 mo), given $E(GM)$ of December 2001 for cycle 23. Regarding $P(AM–AM)$, only 5 of 11 cycles have $P(AM–AM)=126 \pm 6$ mo, with none of the past 3 cycles falling within the bounds. Such a range implies AM for cycle 24 would occur about August 2012 (±6 mo), given E(AM) of February 2002 for cycle 23.

Figure 19 displays the elapsed time in months between the occurrences of GM and RM ($t(GM–RM)$) (fig. 19(a)) and between AM and RM ($t(AM–RM)$) (fig. 19(b)), where negative values indicate parametric leading of $E(RM)$. The medians are 1 and zero, respectively, indicating that GM and AM usually occur closely in time with $E(RM)$. For GM, 9 of 12 cycles have $E(GM)$ within 6 mo of $E(RM)$, with cycles 20, 22, and 23 lagging substantially (19–20 mo). For AM, 10 of 12 cycles have $E(AM)$ within 8 mo of $E(RM)$, with cycles 21 and 23 lagging substantially (22 mo). For both parameters, however, slightly smaller values peaked when RM occurred.

Figure 20 depicts the elapsed time in months between the occurrences of LM and RM ($t(LM–RM)$) (fig. 20(a)) and between HM and RM ($t(HMRM)$) (fig. 20(b)). Again, negative values indicate parametric leading of $E(RM)$. For $t(LM–RM)$, its median is –35.5 mo, and all values are negative, indicating that LM always leads RM. Six of the past 7 cycles have had values shorter than the median (averaging about –26 mo), with 7 of 7 being shorter than –37 mo. Thus, when LM occurs for cycle 24, probably sometime in late 2010, one expects RM to follow within about 2–3 yr.

For $t(HM–RM)$, its median is –15 mo, and all except two cycles (cycles 17 and 22) have had HM leading RM. Six of 12 cycles have HM leading RM by about 15 ± 6 mo. So, again, once HM has been discerned for cycle 24 (unless, of course, cycle 24 happens to behave similarly to cycles 17 and 22), one expects RM to follow within about 1 yr.

Table 3. Periods for selected solar cyclic parameters.

Cycle	*P*(*Rm–Rm*)	*P*(*SM–SM*)	*P*(*Gm–Gm*)	*P*(*Am–Am*)	*P*(*0.5–0.5*)	*P*(*RM–RM*)	*P*(*GM–GM*)	*P*(*AM–AM*)	*P*(*FSD–FSD*)	*P*(*LSD–LSD*)	*P*(*Lm–Lm*)	*P*(*LM–LM*)	*P*(*Hm–Hm*)	*P*(*HM–HM*)
10	135	137	–	–	–	126	–	–	145	135	–	–	–	–
11	141	137	–	–	–	160	–	–	139	170	–	–	–	–
12	135	136	130	134	126	121	114	122	140	99	113	125	116	137
13	142	143	147	143	149	145	149	137	130	163	147	148	151	155
14	139	139	139	139	139	138	137	146	131	135	137	149	138	128
15	120	119	120	120	126	128	131	130	158	117	112	121	109	107
16	121	125	121	121	127	108	106	107	125	108	141	136	139	159
17	125	122	125	127	124	121	127	120	134	122	112	123	116	109
18	122	122	122	120	115	130	124	126	109	121	119	110	128	119
19	126	127	122	126	125	128	147	125	131	130	115	131	117	124
20	140	148	141	145	135	133	108	162	140	131	162	138	149	135
21	123	120	120	118	134	115	140	91	124	120	124	123	123	141
22	116	124	125	116	126	129	130	153	125	126	117	124	119	115
23	(150)	(148)	(147)	(150)	135	–	–	–	117	(137)	143	–	140	–

Table 4. Elapsed time in months relative to $E(Rm)$ for selected solar cyclic parameters.

Cycle	*E*(*Rm*)	*t*(*SM–Rm*)	*t*(*FSD–Rm*)	*t*(*Rm–LSD*)	*t*(*Gm–Rm*)	*t*(*Am–Rm*)	*t*((*A/G*)*m–Rm*)	*t*(*g*(*h*)/*g*>0.5)	*t*(*FHLS–Rm*)	*t*(*Rm–RM*)	*t*(*Lm–Rm*)	*t*(*Hm–Rm*)	*t*(*Rm–LM*)	*t*(*Rm–HM*)	*t*(*LM–RM*)	*t*(*HM–RM*)
10	12–1855	0	–79	28	–	–	–	–	–	50	–	–	–	–	–	–
11	03–1867	2	–65	28	–	–	–	–	–	41	–	–	–	–	–	–
12	12–1878	–2	–67	55	0	0	–5	6	–20	60	–3	–3	14	23	–46	–37
13	03–1890	–1	–62	21	–5	–1	0	–3	–15	46	–25	–22	4	25	–42	–21
14	01–1902	0	–74	42	0	0	–23	4	–24	49	–12	–13	10	37	–39	–11
15	08–1913	0	–82	38	0	0	0	–6	–8	48	–14	–14	8	27	–40	–21
16	08–1923	2	–40	35	0	0	0	0	–22	56	–22	–25	9	14	–47	–42
17	09–1933	0	–36	22	0	0	0	6	–20	43	–2	–7	24	52	–19	9
18	02–1944	0	–27	19	0	2	3	5	–22	39	–15	–16	22	36	–17	–3
19	04–1954	0	–40	18	0	0	1	–2	–3	47	–18	–10	10	33	–37	–14
20	10–1964	1	–35	22	–4	0	0	–3	–12	49	–29	–19	15	31	–34	–18
21	06–1976	–3	–35	13	–3	5	5	–8	–33?	42	–7	–10	13	26	–29	–16
22	09–1986	–6	–34	10	–6	0	0	3	–14?	34	–6	–10	13	44	–21	10
23	05–1996	2	–25	20	3	0	9	13	0	47	–5	–7	21	43	–26	–4
24	11–2008	0	–58	–	0	0	0	–2	–10	–	–18	–17	–	–	–	–

Note: Minus sign means leading *E*(*Rm*) and *E*(*RM*), and the question mark means that the actual time might be slightly shorter.

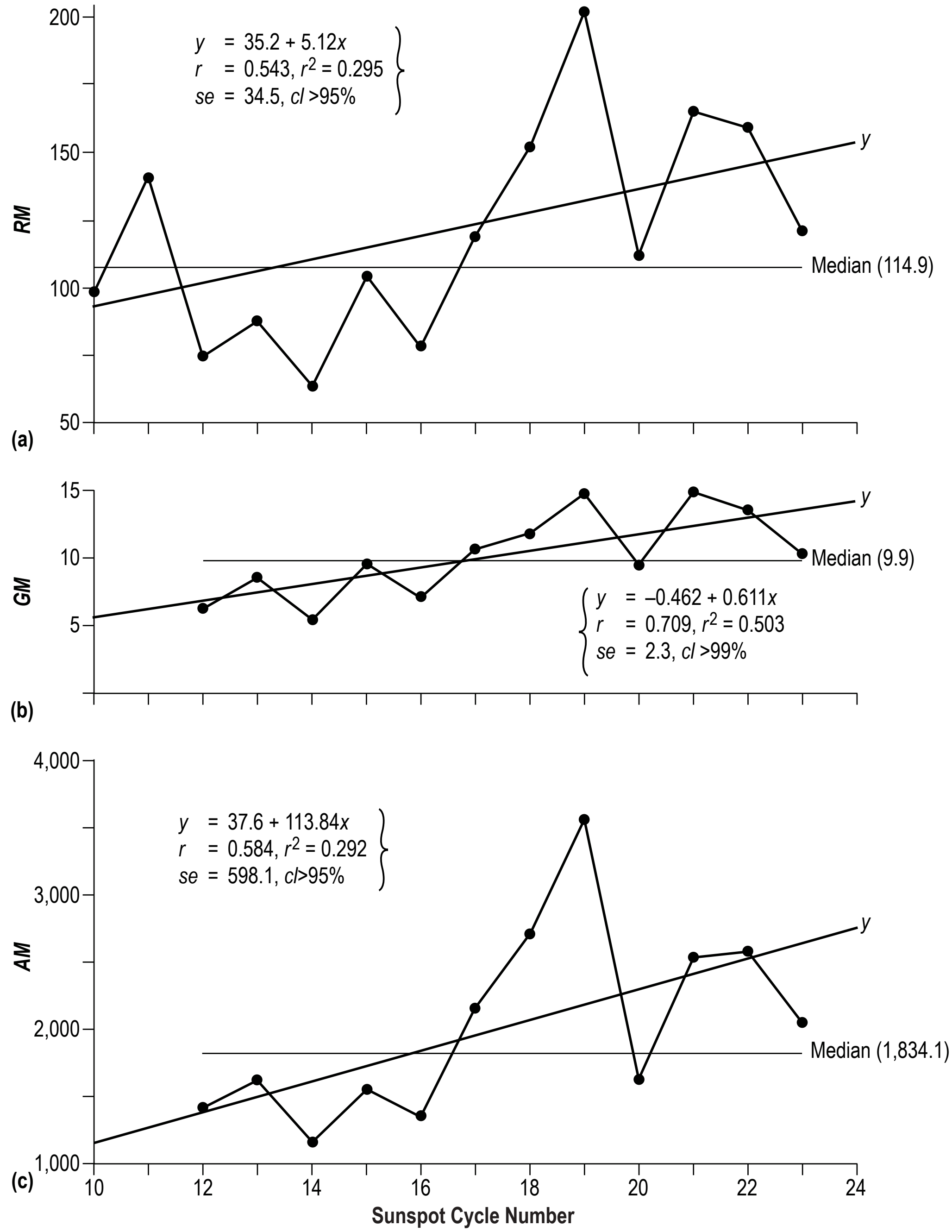

Figure 17. Cyclic variation of (a) *RM*, (b) *GM*, and (c) *AM* for cycles 10–23.

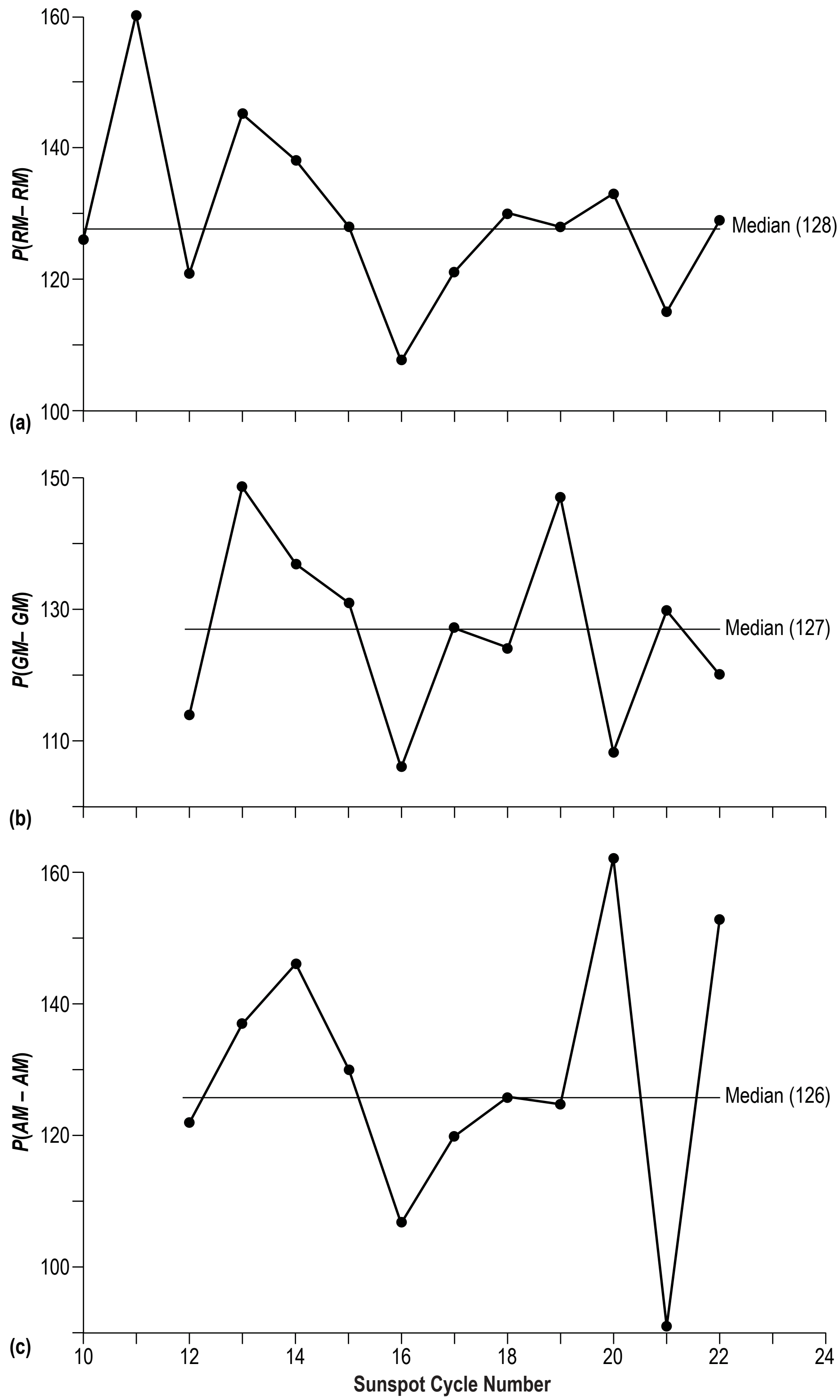

Figure 18. Cyclic variation of (a) $P(RM–RM)$, (b) $P(GM–GM)$, and (c) $P(AM–AM)$ for cycles 10–22.

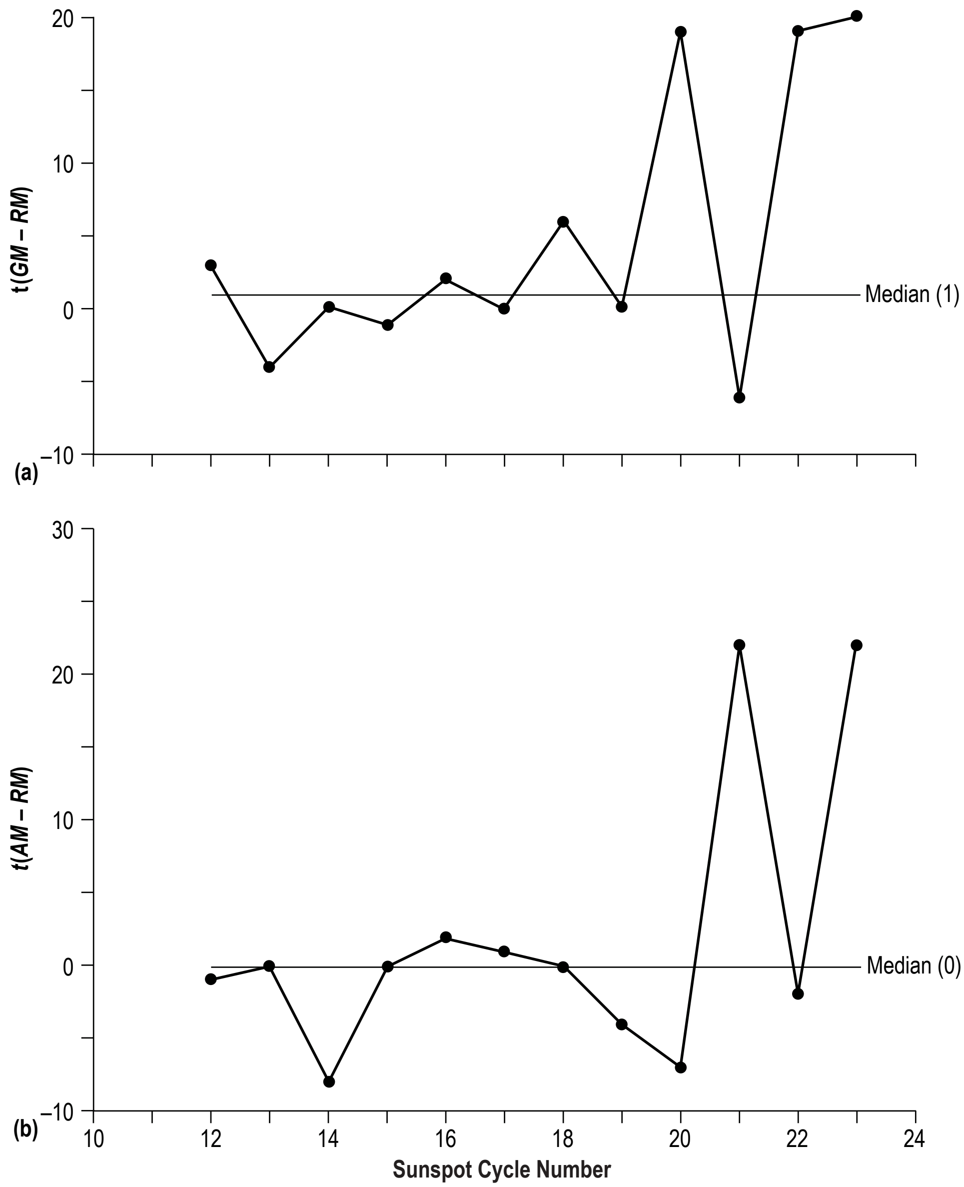

Figure 19. Cyclic variation of (a) $t(GM–RM)$ and (b) $t(AM–RM)$ for cycles 12–23.

2.3 Parametric Comparisons and Correlations

Figure 21 shows the cyclic variation of the elapsed time, in months, between *Rm* and *RM* ($t(Rm–RM)$), which often is simply called the ascent duration (ASC). The median is 47 mo, with 7 of the past 7 cycles having a value of 34–49 mo (averaging about 43 mo). In fact, 11 of 14 cycles have ASC=39–50 mo, with only cycles 22 (ASC=34 mo, the fastest), 12 (ASC=60 mo, the slowest), and 16 (56 mo) having ASCs that fall outside the limits. Because cycle 24's *Rm* is believed to have occurred about November 2008, one strongly expects its *RM* to follow within the next 39–50 mo, implying $E(RM)$ for cycle 24 about February 2012 to January 2013.

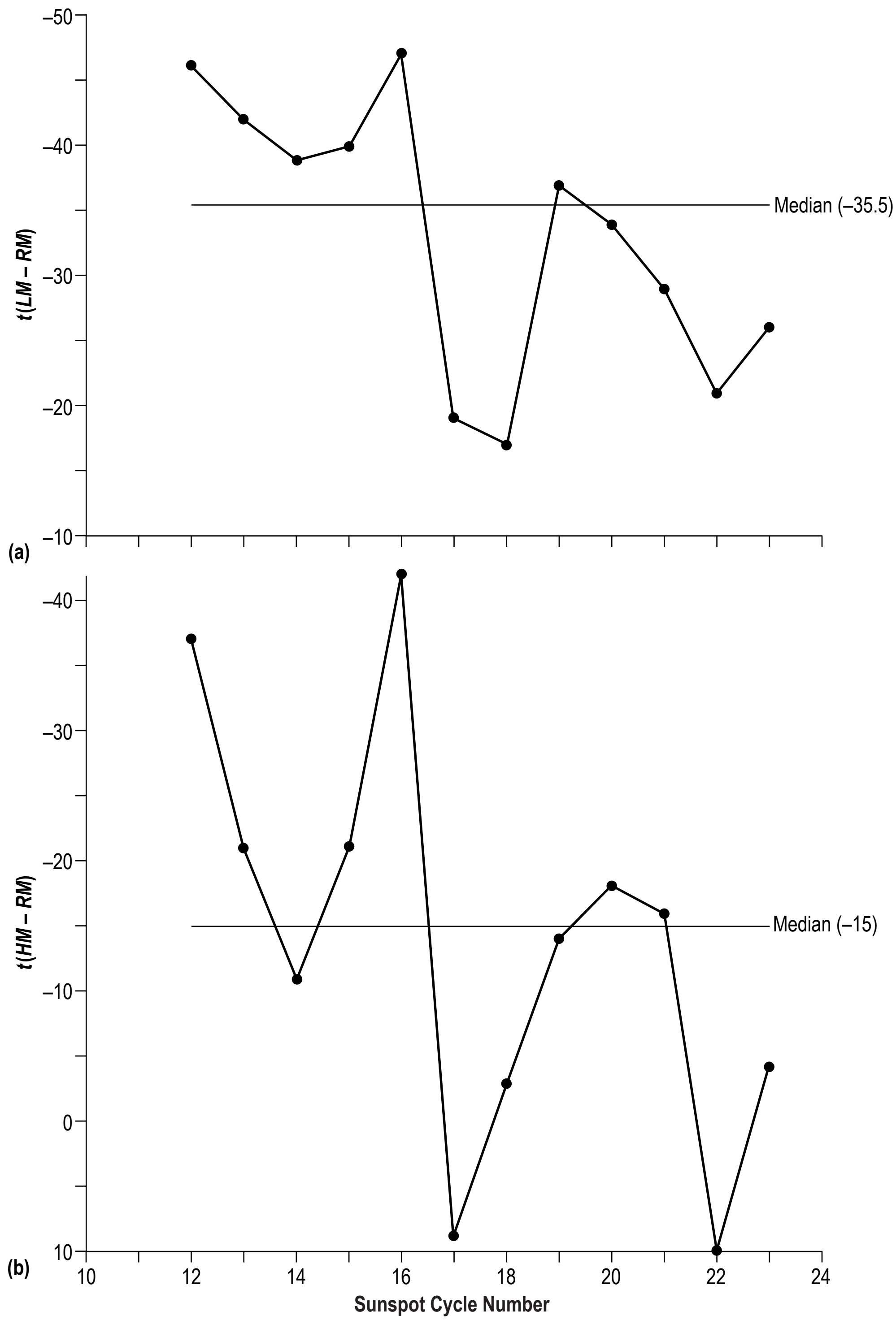

Figure 20. Cyclic variation of (a) $t(LM–RM)$ and (b) $t(HM–RM)$ for cycles 12–23.

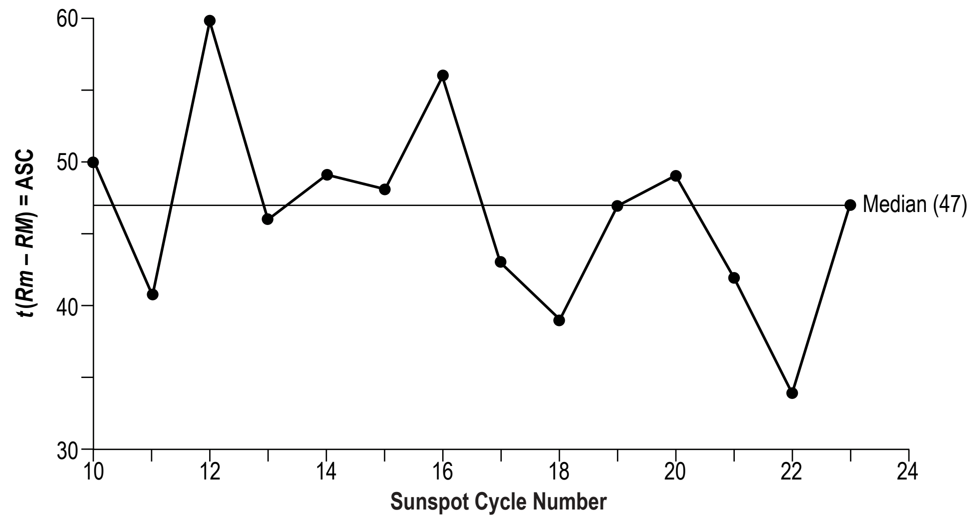

Figure 21. Cyclic variation of $t(Rm–RM)$=ASC for cycles 10–23.

A comparison of *RM* values against ASC produces the well-known Waldmeier effect, where faster-rising cycles tend to be larger-amplitude cycles and slower-rising cycles tend to be smaller-amplitude cycles. Figure 22 displays the Waldmeier effect, both in terms of using ASC as the determining factor and using *RM* as the determining factor. The numbers beside the plotted points are the sunspot cycle numbers. Expressed as a 2×2 contingency table, the probability *P* of obtaining the observed result, or one more suggestive of a departure from independence (chance), is found using Fisher's exact test for 2×2 contingency tables[25] to be 5.1%. Hence, there exists strong statistical evidence that slower-rising cycles tend to be associated with smaller-amplitude cycles (i.e., they tend to populate the lower-right quadrant of the scatter plot), while faster-rising cycles tend to be associated with larger-amplitude cycles (i.e., they tend to populate the upper-left quadrant of the scatter plot). Expressed as regression equations (i.e., performing linear correlation analysis and ignoring cycles 14 and 19, the lower and upper extremes of *RM*, presumed to be statistical outliers), the inferred correlation coefficient is r=–0.884, the coefficient of determination is r^2=0.781 (meaning that more than three-fourths of the variance can be explained by the inferred regressions), and the confidence level of the inferred regressions is *cl* >99.9%. Hence, correlation analysis likewise supports the existence of a strong relationship between *RM* and ASC. Should cycle 24 be a slow riser, one expects its *RM* to be average to lower-than-average size, while, in contrast, should cycle 24 be a fast riser, one expects its *RM* to be average to above-average size. Unfortunately, sunspot cycles usually do not reveal their true character until about 1–2 yr past sunspot minimum.[26–34]

Because sunspot minimum for cycle 24 seems very close at hand and, in fact, may have already occurred in November 2008, the period of cycle 23 (i.e., $P(Rm–Rm)$) can be more accurately gauged, as well as the minimum values of *Rm*, *Gm*, and *Am* for cycle 24. These values can then be used in the amplitude-period[35] and maximum-minimum[12] effects to estimate *RM* for cycle 24. Figure 23 shows the amplitude-period effect for estimating *RM* for an ongoing sunspot cycle using $P(Rm–Rm)$, $P(Gm–Gm)$, $P(Am–Am)$, and $P(SM–SM)$. It compares *RM* for cycle n (the ongoing cycle) against periods for cycle n–1 (the preceding cycle). Based on $P(Rm–Rm)$ and $P(SM–SM)$, Fisher's exact test

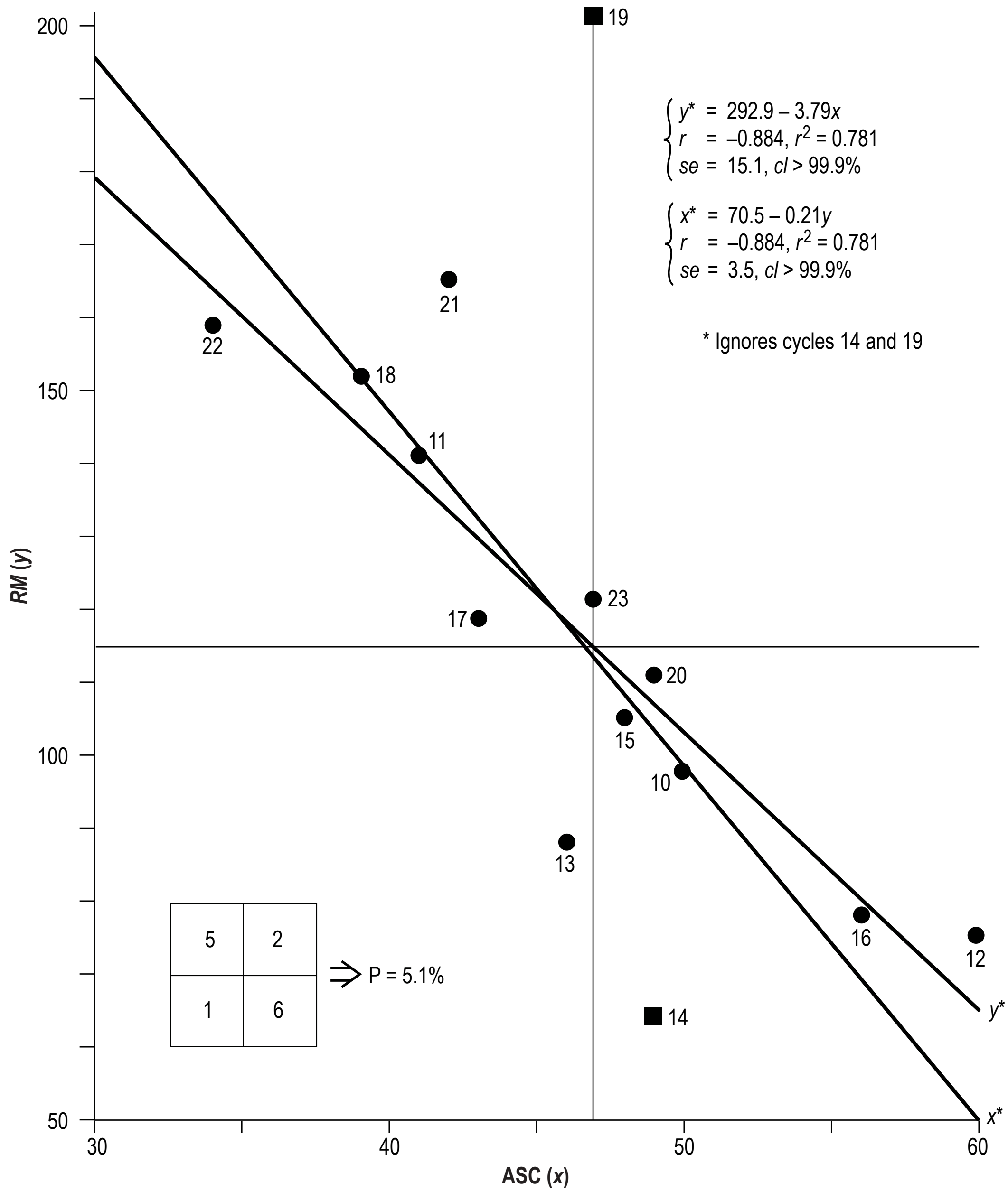

Figure 22. Scatter plot of *RM* versus ASC (the Waldmeier effect).

for 2×2 contingency tables has a probability P of obtaining the observed result, or one more suggestive of a departure from independence, equal to 7.8%. This suggests a marginally statistically significant association between maximum amplitude of the ongoing sunspot cycle and the preceding cycle's period length. Five of 6 preceding cycles of shorter than median period length have had ongoing cycles of larger than median maximum amplitude, and 5 of 7 preceding cycles of longer than median period length have had smaller than median maximum amplitude. Only cycle pairs 10/11, 15/16, and 20/21 fail to adhere to the inferred association pattern. Cycle 23's $P(Rm\text{–}Rm)$ and $P(SM\text{–}SM)$ both measure longer than median period length, suggesting that cycle 24's maximum amplitude probably

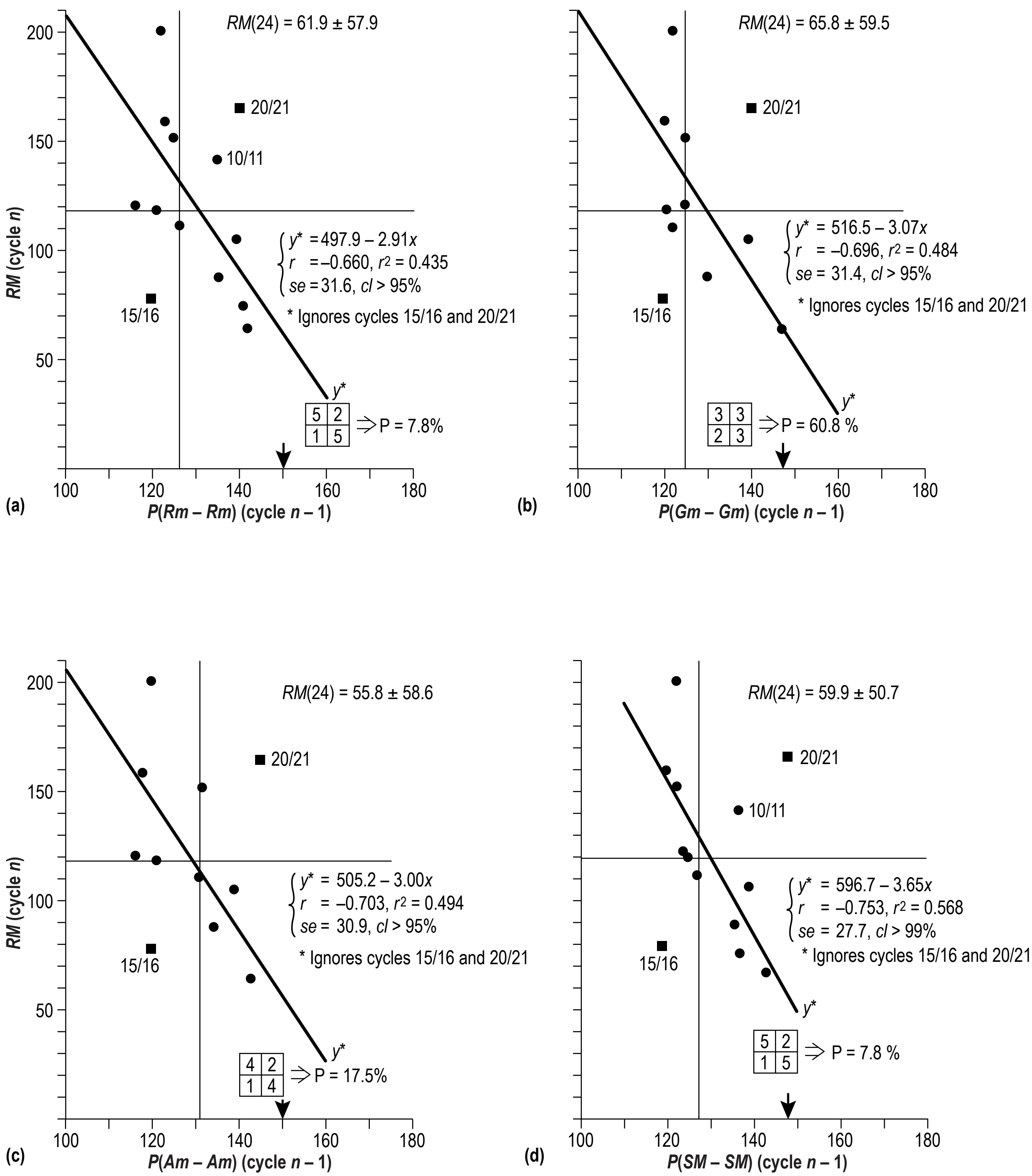

Figure 23. Scatter plots of (a) *RM* (cycle n) versus *P*(*Rm*–*Rm*) (cycle n–1), (b) *RM* (cycle n) versus *P*(*Gm*–*Gm*) (cycle n–1), (c) *RM* (cycle n) versus *P*(*Am*–*Am*) (cycle n–1), and (d) *RM* (cycle n) versus *P*(*SM*–*SM*) (cycle n–1) (the amplitude-period effect).

will be smaller than median size. Less statistically important results are obtained using *P*(*Gm*–*Gm*) and *P*(*Am*–*Am*), which also are based on two fewer cycle pairs.

On the basis of linear correlation analysis, ignoring cycle pairs 15/16 and 20/21 (filled squares), which have the largest deviations from the inferred regression lines, one finds statistically important associations between *RM* and period length for all parametric periods (i.e., *P*(*Rm*–*Rm*), *P*(*Gm*–*Gm*), *P*(*Am*–*Am*), and *P*(*SM*–*SM*)). The most statistically important inferred regression is the one linking *RM* for cycle n with *P*(*SM*–*SM*) for cycle n–1, having $r=-0.753$. Applying cycle 23's *P*(*SM*–*SM*), equal to 147 mo, one computes the 90% prediction interval for cycle 24's *RM* to be 59.9 ± 50.7, inferring only a 5% chance that cycle 24 will have *RM* larger than 110.6. Averaging the four estimates yields an *RM* of about 61 ± 57 for cycle 24, suggesting an upper limit of about 118 for cycle 24.

Figure 24 displays the maximum-minimum effect for estimating *RM* of an ongoing sunspot cycle (cycle 24) using minimum amplitudes: i.e., (a) *Rm*, (b) *Gm*, and (c) *Am*). Again, both Fisher's exact test for 2 × 2 contingency tables and linear correlation analysis (ignoring cycle 19) have been employed in the estimate of *RM* for cycle 24. Based on *Rm*, cycle 24's *RM* is estimated to be about 85 ± 42 (the 90% prediction interval), while, based on *Gm* and *Am*, *RM* for cycle 24 is estimated to be about 83 ± 46 and 98 ± 42, respectively. Averaging the three estimates yields an estimate for cycle 24's *RM* of about 89 ± 43, implying an upper limit of about 132 and a lower limit of about 46 for cycle 24's *RM*. Thus, cycle 24 seems more likely to be a cycle of average to slightly below average size, in contrast to being potentially one of the largest cycles on record.[36–40] Combining the results of the amplitude-period and maximum-minimum effects, the best guess for cycle 24's *RM* is about 82 ± 36.

Figure 25 shows the scatter plots of *RM* versus *HM* (fig. 25(a)), *RM* versus *GM* (fig. 25(b)), and *RM* versus *AM* (fig. 25(c)). All scatter plots are statistically significant, whether expressed as 2 × 2 contingency tables or as *cl*s of inferred regression fits. Hence, by monitoring the monthly values of *H*, *G*, and/or *A*, one can effect monthly projections for *RM*. As an example, *HM* for cycle 24 is expected to lie somewhere in the range of 31–44 deg. Cycles having *HM* less than the median (38.35 deg) usually (5 of 6) have *RM* less than the median (114.9), with all having *RM* ≤119.2. Cycles having *HM* greater than the median usually (5 of 6) have *RM* greater than the median, with all having *RM* ≥105.4. The value of *H* in November 2008 measures about 21 deg, but is continuing to rise. Similarly, cycles having *GM* less than the median (9.91) always (6 of 6) have *RM* less than the median, actually ≤110.6, while cycles having *GM* greater than the median always (6 of 6) have *RM* greater than the median, actually ≥119.2. Cycles having *AM* less than the median (1,834.1) always (6 of 6) have *RM* less than the median, actually ≤110.6, while cycles having *AM* greater than the median always (6 of 6) have *RM* greater than the median, actually ≥119.2.

Interestingly, 10 of 12 cycles fit the paradigm of being larger (or smaller) than median size (114.9) when *H* exceeds (or never exceeds) median value (38.35 deg), failing for cycles 15 (*HM*= 40.5 deg at t=27 mo and *RM*=105.4 at t=48 mo) and 17 (*HM*=36.5 deg at t=52 mo and *RM*=119.2 at 43 mo). The larger than median cycles that fit the paradigm include cycles 18, 19, and 21–23. These cycles had *H* values that first exceeded median value at t=29, 14, 16, 6, and 43 mo, respectively. Hence, if *H* exceeds its median value, especially within the first 1–2 yr following *E*(*Rm*), one very probably expects the cycle to be larger than median size. Applying the Spearman rank correlation test[41] to cycles 18, 19, and 21–23 (ranking the t values when *H* first exceeded median value and

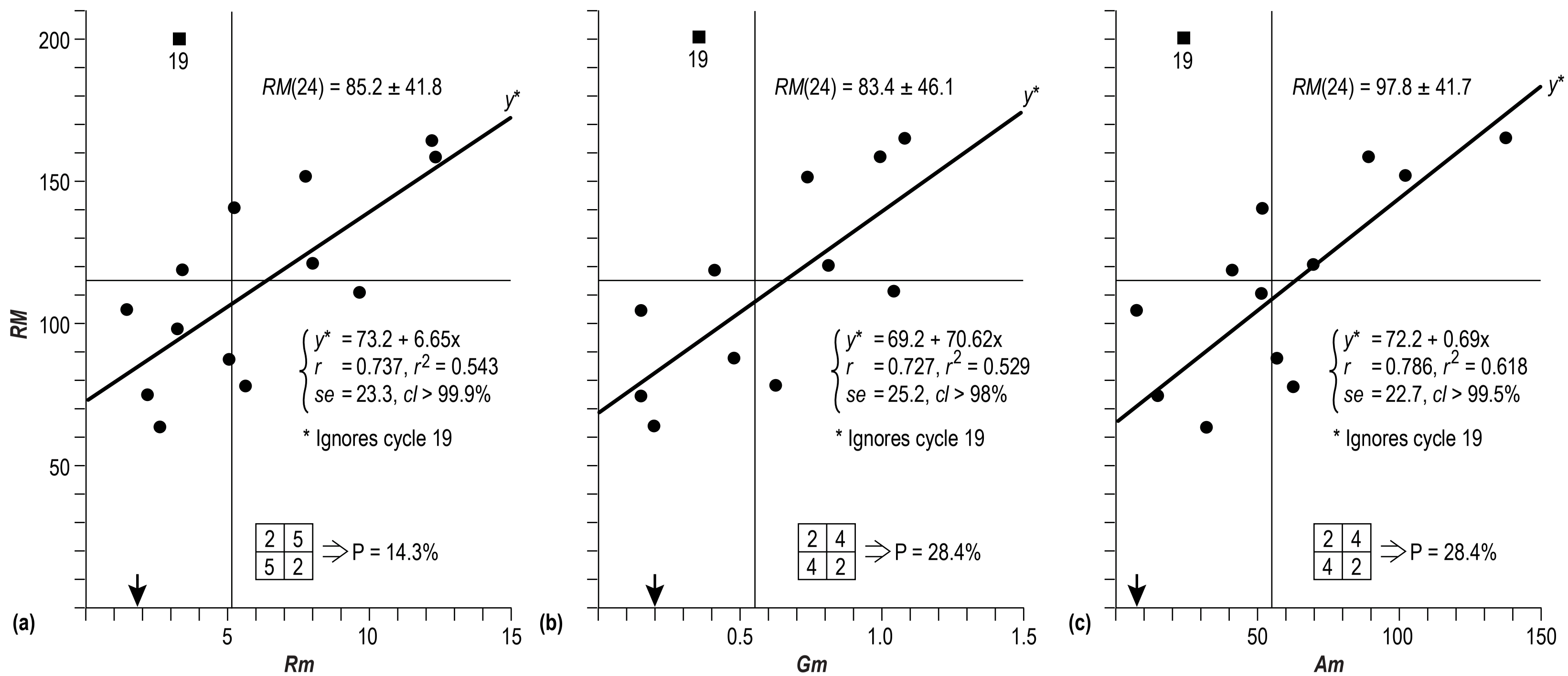

Figure 24. Scatter plots of (a) *RM* versus *Rm*, (b) *RM* versus *Gm*, and (c) *RM* versus *Am* (the maximum-minimum effect).

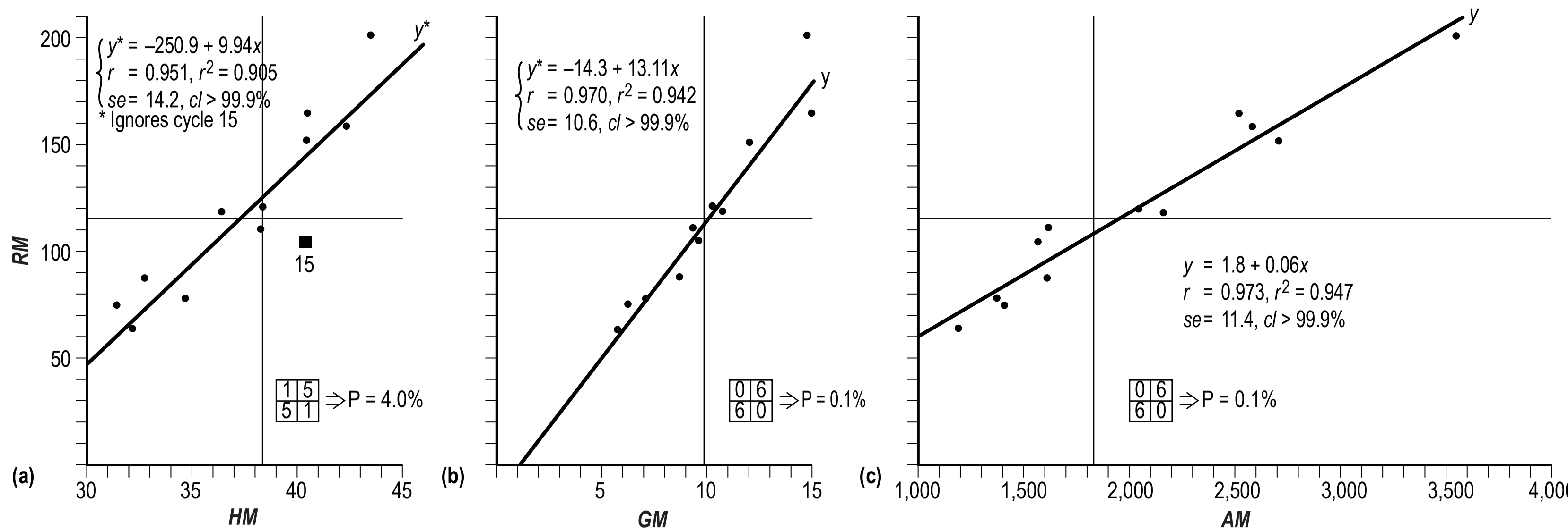

Figure 25. Scatter plots of (a) *RM* versus *HM*, (b) *RM* versus *GM*, and (c) *RM* versus *AM*.

the later occurring RM values) hints of an almost marginally significant inverse association between the two parameters, such that the quicker that H exceeds its median maximum value, the larger the expected maximum amplitude for the cycle.

Figure 26(a) displays the scatter plot of HM versus Hm for cycles 12–23, with the arrow representing the Hm value for cycle 24. Given are the results of Fisher's exact test for 2×2 contingency tables and correlation analysis, ignoring cycles 15 and 16 (the filled squares). The measured value of Hm for cycle 24 (11.7 deg in June 2007) suggests that cycle 24 probably will fall short of median value (38.35 deg), having an expected value of about 35.0 ± 4.6 deg (the 90% prediction interval). Consequently, cycle 24 is expected to have an RM of only average to below-average size (i.e., about 97 ± 46, applying the value of 35.0 ± 4.6 deg to the inferred regression given in fig. 25(a)) rather than average to above-average size.

Figure 26(b) gives the mean variation of cycles 12–23 for elapsed time in months from $E(Rm)$ to 30 mo past $E(Rm)$ based on superposed epoch analysis. Also shown for comparison are the values of H from $E(Rm)$ for cycles 14 (the smallest cycle of the modern era) and 19 (the largest cycle of the modern era, as well as the H values for cycles 12–24 at $E(Rm)$, where cycle 24's H value at $E(Rm)$ is marked by a small arrow and presumes $E(Rm)$ in November 2008. The value of H at $E(Rm)$ for cycle 24 plainly is lower than the mean at $E(Rm)$ and is in the middle range of H values at $E(Rm)$. HM values for cycles 12–23 are also displayed. It is apparent that if cycle 24 is destined to be a larger-amplitude cycle, its H must rapidly increase in value within the first year or so, rising above the mean of cycles 12–23. If it does not rise rapidly exceeding the mean, it seems highly unlikely that cycle 24 will be a larger-amplitude cycle.

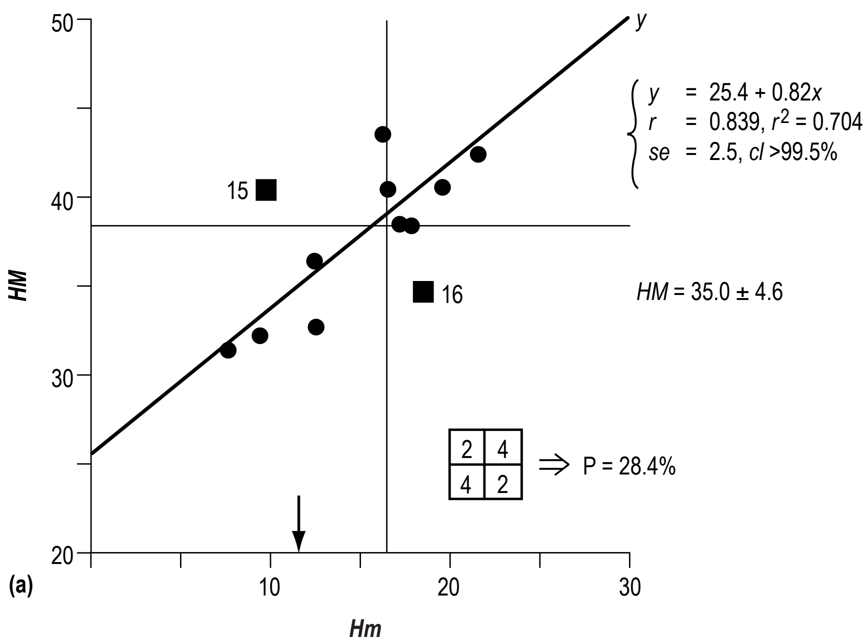

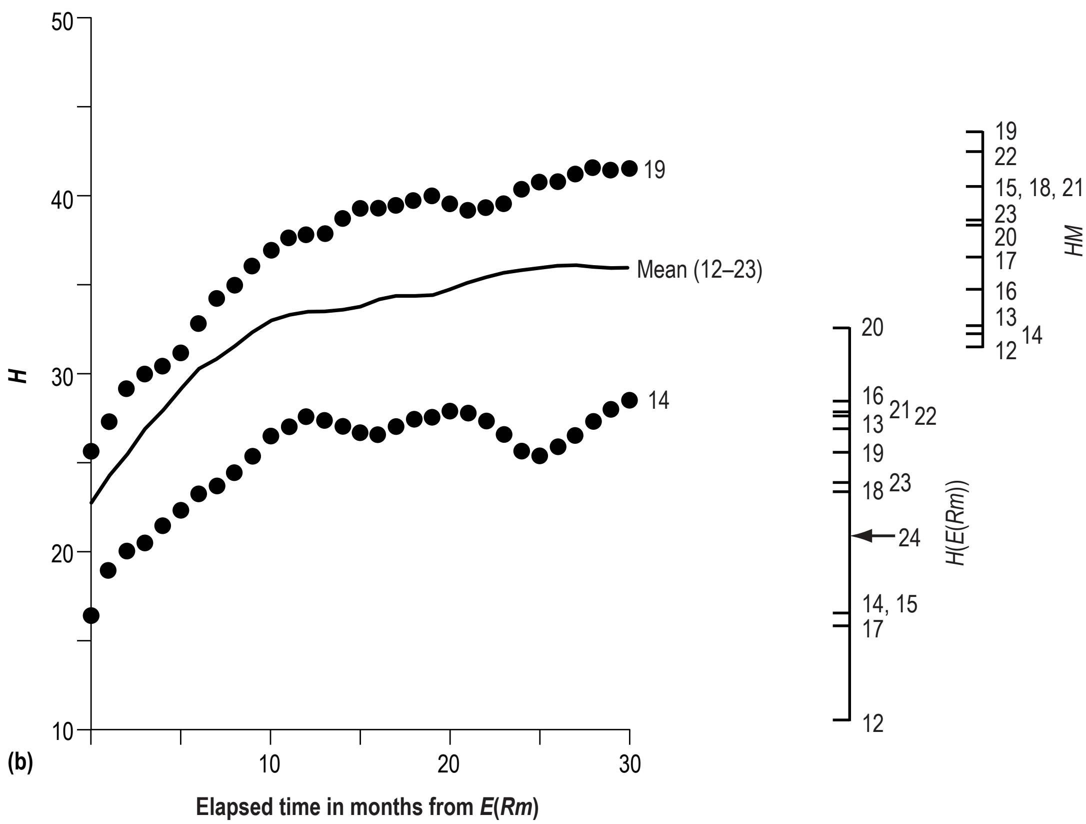

Figure 26. Values of H: (a) Scatter plot of HM versus Hm, and (b) superposed epoch analysis of H for elapsed time 0–30 mo from $E(Rm)$, giving mean of cycles 12–23 and H values for cycles 14 and 19, the smallest and largest modern era cycles, respectively.

3. SUMMARY

Twelve-mma values of cyclic parameters (e.g., *S*, *R*, *G*, *A*, and *A*/*G*) are reflective of cyclic minimum conditions in late 2008. Presuming sunspot minimum in November 2008 (*Rm* ≈1.8), cycle 23 has a minimum-to-minimum length of 150 mo, the longest of all modern era sunspot cycles (from cycle 10). The first spotless day after cycle maximum for cycle 23 and before the start of cycle 24 occurred in January 2004; the first true new-cycle, high-latitude spot occurred in January 2008; and the monthly mean number of new-cycle groups first dominated the monthly mean number of old-cycle groups in September 2008. The 12-mma values of *L* and *H* were at minimum value in May and June 2007, respectively, with current values of *L* and *H* continuing to rise. The overlap of cycles 23–24 now spans at least 16 mo (from January 2008 through April 2009), but will possibly be longer if old-cycle spots continue to be seen later in 2009 (overlapping of 1–4 yr has been seen in previous cycles based on *FHLS* and *LLLS* determinations).

Spotless days have continued to be seen through at least August 2009, now spanning at least 68 mo. If the current period of spotless days (i.e., *t*(*FSD*–*LSD*)) is more akin to those for early cycles 10–15 than more recent cycles 16–23, spotless days will continue to be seen for at least another year or more, perhaps another 2–3 yr. In November 2008, the 12-mma of *S* measured 24.2, which is the fourth highest number, close to but below that for cycles 12 (25.0), 14 (24.3), and 15 (26.2). Because *SM* closely associates with the occurrence of *Rm*, having occurred simultaneously with *Rm* for 6 of 14 cycles and within 2 mo of *Rm* for 12 of 14 cycles (failing for cycles 21 and 22, with *SM* leading *Rm* by 3 and 6 mo, respectively, for these cycles) and because of the recent increase in solar activity in early July 2009, the minimum for cycle 24 is expected to be established in late 2008 (probably November or December 2008).

Cycle 23 is now known to be a cycle of longer period, more akin to early cycles 10–14 and 20 rather than to cycles 15–19, 21, and 22, which are of shorter period. On the basis of *P*(*Lm*–*Lm*) and *P*(*Hm*–*Hm*), cycle 23 could have been projected to be a cycle of longer period some time ago, since *Lm* and *Hm* usually occur well before *Rm*. Previously, 4 of 5 cycles of longer than median *P*(*Lm*–*Lm*) or *P*(*Hm*–*Hm*) have been cycles of longer period, as determined using *R* (i.e., *P*(*Rm*–*Rm*), and 6 of 7 cycles of shorter than median *P*(*Lm*–*Lm*) or *P*(*Hm*–*Hm*) have been cycles of shorter period as determined using *R*. Only cycles 12 and 16 failed to agree with this paradigm.

While cycles are generally believed to average about 11 yr in length between minimum occurrences using 12-mma of *R*, the distribution of cycle lengths clearly is better described as bimodal, consisting of shorter and longer period cycles with an 8-mo gap separating the lower and upper extremes of the inferred cyclic groupings. While true, interestingly, the length of individual cycles as determined using *t*(*FHLS*–*LLLS*) has a median of 162 mo, ranging between 142 and 190 mo, suggesting, perhaps, that the real average length of an individual sunspot cycle—i.e., from its *FHLS* to its *LLLS*—is much longer than that found using sunspot number. Perhaps it is the strength of the following new cycle (i.e., the rapidity of new cycle spot formation and manifestation) that determines the apparent period of the just-ending old cycle (i.e., being either of shorter or longer period as determined from R). Based on R, the overlap of old and new cycles is about 1–4 yr (often 3 yr), with the shortest overlap (about 16 mo) being associated with the ending of cycle 18 and the beginning of cycle 19, the largest cycle of the modern era. The current overlap for cycles 23/24 measures at least 16 mo through April 2009 (no old-cycle, near-equatorial spots were seen in May or June 2009).

Current values for the period of cycle 23 (≈150 mo) and the minimum amplitude (≈1.8) of cycle 24 can be used in the amplitude-period and maximum-minimum effects to estimate the size of cycle 24. Both strongly suggest that cycle 24 will be a cycle of average to below-average size, unless it proves to be a statistical outlier. Furthermore, an average to below-average size cycle suggests an average to slower-than-average ASC (from the Waldmeier effect) for cycle 24. Consequently, given minimum amplitude for cycle 24 in late 2008, one anticipates its maximum amplitude in late 2012 to early 2013, unless, again, cycle 24 proves to be a statistical outlier. The longer cycle 23 persists, the greater the chance that cycle 24 will be only of average to below-average size. There is only about a 1% chance that cycle 23 will persist 155 mo or more, implying $E(Rm)$ for cycle 24 on or before April 2009.

Continuous monitoring of H, G, and A will provide strong evidence as to whether cycle 24 will be only of average to below-average size or larger-than-average size. For example, should H exceed 38.35 deg during its rise from minimum to maximum, one expects cycle 24 to be of larger amplitude. The same is true should G and A exceed their median maximum values (9.9 and 1,834.1, respectively). The value of H in November 2008 measures only ≈21 deg (up from its minimum value of 11.7 deg in June 2007), but is continuing to rise, with maximum value expected within the next 1–2 yr. If H does not exceed median maximum value, then one expects RM for cycle 24 to be only of average to below-average size. Based on the inferred relationship between HM and Hm (ignoring cycles 15 and 16), one expects HM for cycle 24 to measure about 35.0 ± 4.6 deg (the 90% prediction interval). Surprisingly, there is a hint that the quicker that HM exceeds the median, the larger the expected size of the cycle; e.g., cycles 19, 21, and 22, the three largest cycles of the modern era, exceeded median value in only 6–16 mo from $E(Rm)$. So, it is with great anticipation that solar prognosticators await the unveiling of cycle 24. Will it be a statistical outlier and thus be larger than expected from the amplitude-period and maximum-minimum effects, suggesting a continuing rise of the secular trend (RM=158.1 ± 34.5, ± 1σ accuracy)? Or, has the trend now reversed and cycle 24 can be expected to, instead, be part of a long-term downward trend over the next several sunspot cycles? Only time will tell.

REFERENCES

1. Schwabe, H.: "Sonnen-Beobachtungen im Jahre 1843," *Astron. Nach*., Vol. 21, p. 233, 1844.

2. Kiepenheuer, K.O.: "Solar Activity," in *The Sun*, Vol. I, *The Solar System*, G.P. Kuiper (ed.), The University of Chicago Press, Chicago, p. 322, 1953.

3. Wilson, R.M.: "A Comparison of Wolf's Reconstructed Record of Annual Sunspot Number with Schwabe's Observed Record of 'Clusters of Spots' for the Interval of 1826-1868," *Solar Phys*., Vol. 182, p. 217, 1998.

4. Bray, R.J.; and Loughhead, R.E.: *Sunspots*, John Wiley & Sons, Inc., New York, p. 4, 1964.

5. Hoyt, D.V.; and Schatten, K.H.: *The Role of the Sun in Climate Change*, Oxford University Press, New York, p. 34, 1997.

6. Waldmeier, M.: *The Sunspot-Activity in the Years 1610-1960*, Swiss Federal Observatory, Schulthess & Co., Zürich, p. 5, 1961.

7. Eddy, J.A.: "The Historical Record of Solar Activity," in *The Ancient Sun: Fossil Record in the Earth, Moon and Meteorites*, R.O. Pepin, J.A. Eddy and R.B. Merrill (eds.), Pergamon Press, New York, p. 119, 1980.

8. McKinnon, J.A.: "Sunspot Numbers: 1610-1985, based on 'The Sunspot-Activity in the Years 1610-1960'," *Report UAG-95*, World Data Center A for Solar-Terrestrial Physics, Boulder, Colorado, p. 1, January 1987.

9. Bruzek, A.: "8. Spots and Faculae," in *Illustrated Glossary for Solar and Solar-Terrestrial Physics*, A. Bruzek and C.J. Durrant (eds.), D. Reidel Publ. Co., Dordrecht, Holland, p. 71, 1977.

10. Wilson, R.M.; and Hathaway, D.H.: "A Comparison of Rome Observatory Sunspot Area and Sunspot Number Determinations with International Measures, 1958–1998," *NASA/TP-2005-214191*, Marshall Space Flight Center, Alabama, 20 pp., November 2005, available online at <http://trs.nis.nasa.gov/archive/00000716/>.

11. Wilson, R.M.; and Hathaway, D.H.: "On the Relation between Sunspot Area and Sunspot Number," *NASA/TP-2006-214324*, Marshall Space Flight Center, Alabama, 20 pp., February 2006, available online at <http://trs.nis.nasa.gov/archive/00000724/>.

12. Hathaway, D.H.; Wilson, R.M.; and Reichmann, E.J.: "Group Sunspot Numbers: Sunspot Cycle Characteristics," *Solar Phys*., Vol. 211, p. 357, 2002.

13. Wilson, R.M.: "On the Distribution of Sunspot Cycle Periods," *J. Geophys. Res*., Vol. 92, p. 10,101, 1987.

14. Harvey, K.L; and White, O.R.: “What is Solar Minimum?” *J. Geophys. Res.*, Vol. 104, p. 19,759, 1999.

15. Maunder, E. W.: “Note on the Distribution of Sun-Spots in Heliographic Latitude, 1874-1902,” *Mon. Not. Roy. Astron. Soc.*, Vol. 64, p. 747, 1904.

16. Wilson, R.M.; Hathaway, D.H.; and Reichmann, E.J.: “On the Behavior of the Sunspot Cycle near Minimum,” *J. Geophys. Res.*, Vol. 101, p. 19,967, 1996.

17. Wilson, R.M.; Hathaway, D.H.; and Reichmann, E.J.: “Gauging the Nearness and Size of Cycle Minimum,” *NASA/TP-3674*, Marshall Space Flight Center, Alabama, 20 pp., February 1997, available online at <http://trs.nis.nasa.gov/archive/00000366/>.

18. Wilson, R.M.: “On the Prospect of Using Butterfly Diagrams to Predict Cycle Minimum,” *Solar Phys.*, Vol. 111, p. 255, 1987.

19. Wilson, R.M.; and Hathaway, D.H.: “Anticipating Cycle 24 Minimum and Its Consequences: An Update,” NASA/TP-2008-215576, Marshall Space Flight Center, Alabama, 44 pp., October 2008, available online at <http://trs.nis.nasa.gov/archive/00000793/>.

20. Wilson, R.M.: “On the Use of ‘First Spotless Day’ as a Predictor for Sunspot Minimum,” *Solar Phys.*, Vol. 158, p. 197, 1995.

21. Wilson, R.M.; and Hathaway, D.H.: “On the Relation between Spotless Days and the Sunspot Cycle,” *NASA/TP-2005-213608*, Marshall Space Flight Center, Alabama, 32 pp., January 2005, available online at <http://trs.nis.nasa.gov/archive/00000695/>.

22. Wilson, R.M.; and Hathaway, D.H.: “On the Relationship between Spotless Days and the Sunspot Cycle: A Supplement,” *NASA/TP-2006-214601*, Marshall Space Flight Center, Alabama, 64 pp., August 2006, available online at <http://trs.nis.nasa.gov/archive/00000735/>.

23. Wilson, R.M.; and Hathaway, D.H.: “Anticipating Cycle 24 Minimum and Its Consequences,” *NASA/TP-2007-215134*, Marshall Space Flight Center, Alabama, 50 pp., November 2007, available online at <http://trs.nis.nasa.gov/archive/00000768/ >.

24. Wilson, R.M., “On the Long-Term Secular Increase in Sunspot Number,” *Solar Phys.*, Vol. 115, p. 397, 1988.

25. Everitt, B.S.: *The Analysis of Contingency Tables*, John Wiley & Sons, New York, p. 15, 1977.

26. Wilson, R.M., “Predicting the Maximum Amplitude for the Sunspot Cycle from the Rate of Rise in Sunspot Number,” *Solar Phys.*, Vol. 117, p. 179, 1988.

27. Wilson, R.M., “On the Average Rate of Growth in Sunspot Number and the Size of the Sunspot Cycle,” *Solar Phys.*, Vol. 125, p. 133, 1990.

28. Wilson, R. M., “On the Maximum Rate of Change in Sunspot Number Growth and the Size of the Sunspot Cycle,” *Solar Phys.*, Vol. 127, p. 199, 1990.

29. Hathaway, D.H.; Wilson, R.M.; and Reichmann, E.J.: "The Shape of the Sunspot Cycle," *Solar Phys.*, Vol. 151, p. 177, 1994.

30. Hathaway, D.H.; Wilson, R.M.; and Reichmann, E.J.: "A Survey and Synthesis of Solar Cycle Prediction Techniques," *J. Geophys. Res.*, Vol. 104, p. 22,375, 1999.

31. Wilson, R.M.; Hathaway, D.H.; and Reichmann, E.J.: "On the Correlation between Maximum Amplitude and Smoothed Monthly Mean Sunspot Number during the Rise of the Cycle (from t=0-48 Months Past Sunspot Minimum)," *NASA/TP-1998-208591*, Marshall Space Flight Center, Alabama, 20 pp., August 1998, available online at <http://trs.nis.nasa.gov/archive/00000458/>.

32. Wilson, R.M.; and Hathaway, D.H.: "Application of the Maximum Amplitude-Early Rise Correlation to Cycle 23," *NASA/TP-2004-213281*, Marshall Space Flight Center, Alabama, 24 pp., June 2004, available online at <http://trs.nis.nasa.gov/archive/00000674/>.

33. Wilson, R.M.; and Hathaway, D.H.: "An Examination of Sunspot Number Rates of Growth and Decay in Relation to the Sunspot Cycle," *NASA/TP-2006-214433*, Marshall Space Flight Center, Alabama, 32 pp., June 2006, available online at <http://trs.nis.nasa.gov/archive/00000731/>.

34. Wilson, R.M.; and Hathaway, D.H.: "Using the Inflection Points and Rates of Growth and Decay to Predict Levels of Solar Activity," *NASA/TP-2008-215473*, Marshall Space Flight Center, Alabama, 48 pp., September 2008, available online at <http://trs.nis.nasa.gov/archive/00000787/>.

35. Wilson, R.M.; and Hathaway, D.H.: "On the Period-Amplitude and Amplitude-Period Relationships," *NASA/TP-2008-215580*, Marshall Space Flight Center, Alabama, 20 pp., November 2008, available online at <http://trs.nis.nasa.gov/archive/00000794/>.

36. Dikpati, M.; de Toma, G.; and Gilman, P.A.: "Predicting the Strength of Solar Cycle 24 Using a Flux-Transport Dynamo-Based Model," *Geophys. Res. Lett.*, Vol. 33, p. L05102, 2006.

37. Hathaway, D.H.; and Wilson, R.M.: "Geomagnetic Activity Indicates Large Amplitude for Sunspot Cycle 24," *Geophys. Res. Lett.*, Vol. 33, p. L18101, 2006.

38. Wilson, R.M.; and Hathaway, D.H.: "An Examination of Selected Geomagnetic Indices in Relation to the Sunspot Cycle," NASA/TP-2006-214711, Marshall Space Flight Center, Alabama, 52 pp., December 2006, available online at <http://trs.nis.nasa.gov/archive/00000741/>.

39. Wilson, R.M.; and Hathaway, D.H.: "Using the Modified Precursor Method to Estimate the Size of Cycle 24," *NASA/TP-2008- 215467*, Marshall Space Flight Center, Alabama, 44 pp., July 2008, available online at <http://trs.nis.nasa.gov/archive/00000789/>.

40. Svalgaard, L.; Cliver, E.W.; and Kamide, Y.: "Sunspot Cycle 24: Smallest Cycle in 100 years?" *Geophys. Res. Lett.*, Vol. 32, p. L01104, 2005.

41. Langley, L.: *Practical Statistics Simply Explained*, revised edition, Dover Publ., New York, p. 199, 1971.

REPORT DOCUMENTATION PAGE						*Form Approved* *OMB No. 0704-0188*

1. REPORT DATE *(DD-MM-YYYY)* 01–09–2009	**2. REPORT TYPE** Technical Publication	**3. DATES COVERED** *(From - To)*

4. TITLE AND SUBTITLE Sunspot Activity Near Cycle Minimum and What It Might Suggest for Cycle 24, the Next Sunspot Cycle	**5a. CONTRACT NUMBER**
	5b. GRANT NUMBER
	5c. PROGRAM ELEMENT NUMBER
6. AUTHOR(S) Robert M. Wilson and David H. Hathaway	**5d. PROJECT NUMBER**
	5e. TASK NUMBER
	5f. WORK UNIT NUMBER
7. PERFORMING ORGANIZATION NAME(S) AND ADDRESS(ES) George C. Marshall Space Flight Center Marshall Space Flight Center, AL 35812	**8. PERFORMING ORGANIZATION REPORT NUMBER** M–1267
9. SPONSORING/MONITORING AGENCY NAME(S) AND ADDRESS(ES) National Aeronautics and Space Administration Washington, DC 20546–0001	**10. SPONSORING/MONITOR'S ACRONYM(S)**
	11. SPONSORING/MONITORING REPORT NUMBER NASA/TP—2009–216061

12. DISTRIBUTION/AVAILABILITY STATEMENT
Unclassified-Unlimited
Subject Category 92
Availability: NASA CASI (443–757–5802)

13. SUPPLEMENTARY NOTES
Prepared by the Science and Mission Systems Office, Science and Exploration Research Office

14. ABSTRACT
In late 2008, 12-month moving averages of sunspot number, number of spotless days, number of groups, area of sunspots, and area per group were reflective of sunspot cycle minimum conditions for cycle 24, these values being of or near record value. The first spotless day occurred in January 2004 and the first new-cycle, high-latitude spot was reported in January 2008, although old-cycle, low-latitude spots have continued to be seen through April 2009, yielding an overlap of old and new cycle spots of at least 16 mo. New-cycle spots first became dominant over old-cycle spots in September 2008. The minimum value of the weighted mean latitude of sunspots occurred in May 2007, measuring 6.6 deg, and the minimum value of the highest-latitude spot followed in June 2007, measuring 11.7 deg. A cycle length of at least 150 mo is inferred for cycle 23, making it the longest cycle of the modern era. Based on both the maximum-minimum and amplitude-period relationships, cycle 24 is expected to be only of average to below-average size, peaking probably in late 2012 to early 2013, unless it proves to be a statistical outlier.

15. SUBJECT TERMS
Sun, sunspot cycle, solar activity, solar cycle prediction, solar cycle 24, latitudinal distribution of spots, maximum-minimum effect, amplitude-period effect

16. SECURITY CLASSIFICATION OF: a. REPORT	b. ABSTRACT	c. THIS PAGE	**17. LIMITATION OF ABSTRACT**	**18. NUMBER OF PAGES**	**19a. NAME OF RESPONSIBLE PERSON** STI Help Desk at email: help@sti.nasa.gov
U	U	U	UU	60	**19b. TELEPHONE NUMBER** *(Include area code)* STI Help Desk at: 443-757-5802

National Aeronautics and
Space Administration
IS20
George C. Marshall Space Flight Center
Marshall Space Flight Center, Alabama
35812